Supporting Information

Antibacterial Azaphilones from an Endophytic Fungus *Colletotrichum* sp. BS4

Wen-Xuan Wang,[†] Souvik Kusari,*[,†] Hartmut Laatsch,[‡] Christopher Golz,[§] Parijat Kusari,[⊥] Carsten Strohmann,[§] Oliver Kayser,[⊥] Michael Spiteller*[,†]

[†]Institute of Environmental Research (INFU), Department of Chemistry and Chemical Biology, Chair of Environmental Chemistry and Analytical Chemistry, TU Dortmund, Otto-Hahn-Straße 6, D-44221 Dortmund, Germany

[‡]Institute for Organic and Biomolecular Chemistry, Georg-August University, Tammannstrasse 2, D-37077 Göttingen, Germany

[§]Inorganic Chemistry, Department of Chemistry and Chemical Biology, TU Dortmund, Otto-Hahn-Straße 6, D-44221 Dortmund, Germany

[⊥]Department of Biochemical and Chemical Engineering, Chair of Technical Biochemistry, TU Dortmund, Emil-Figge-Straße 66, D-44227 Dortmund, Germany

Table of contents

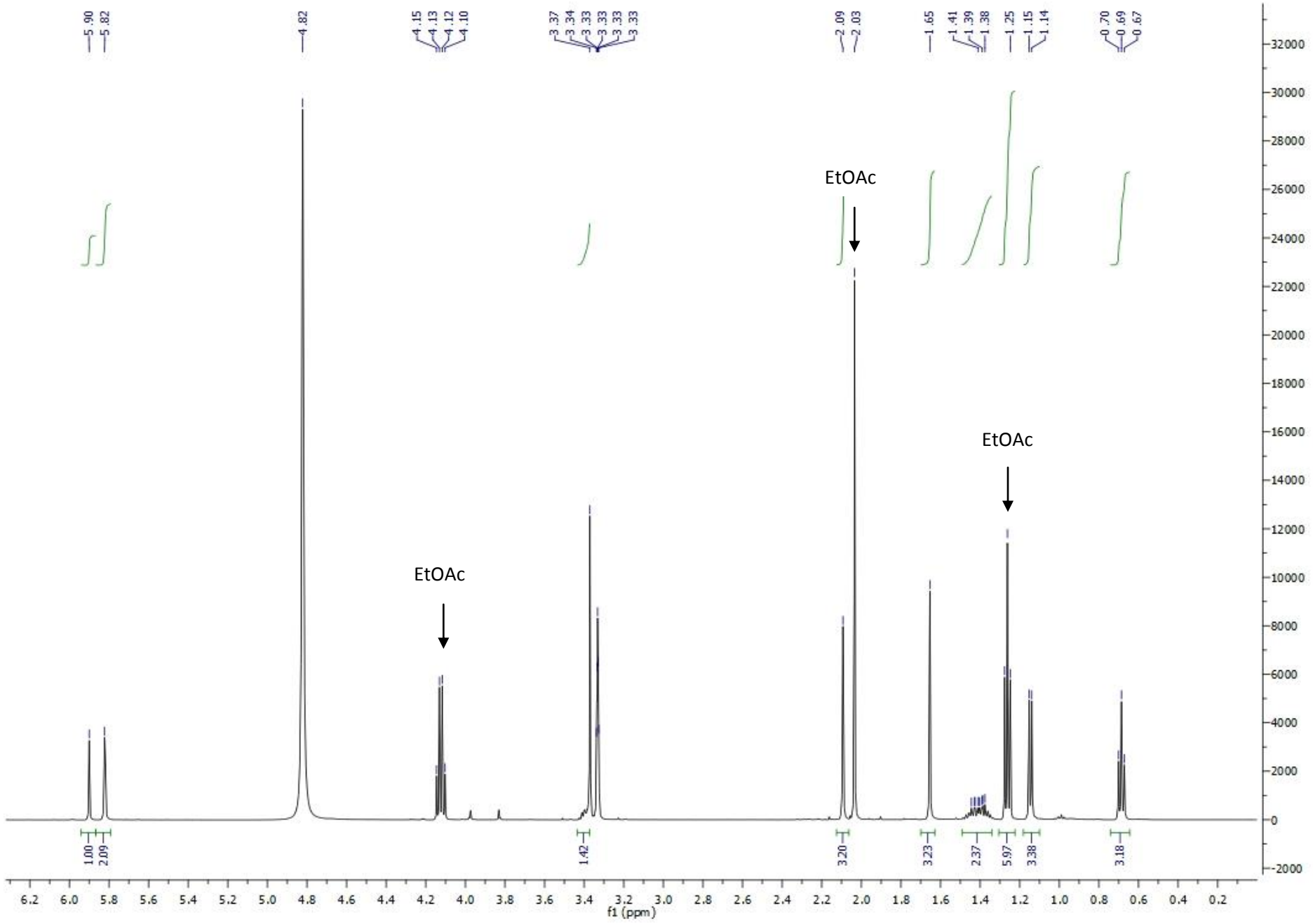

Figure S1. ^{1}H NMR (500 MHz, CD_3OD) spectrum of colletotrichone A (**1**)

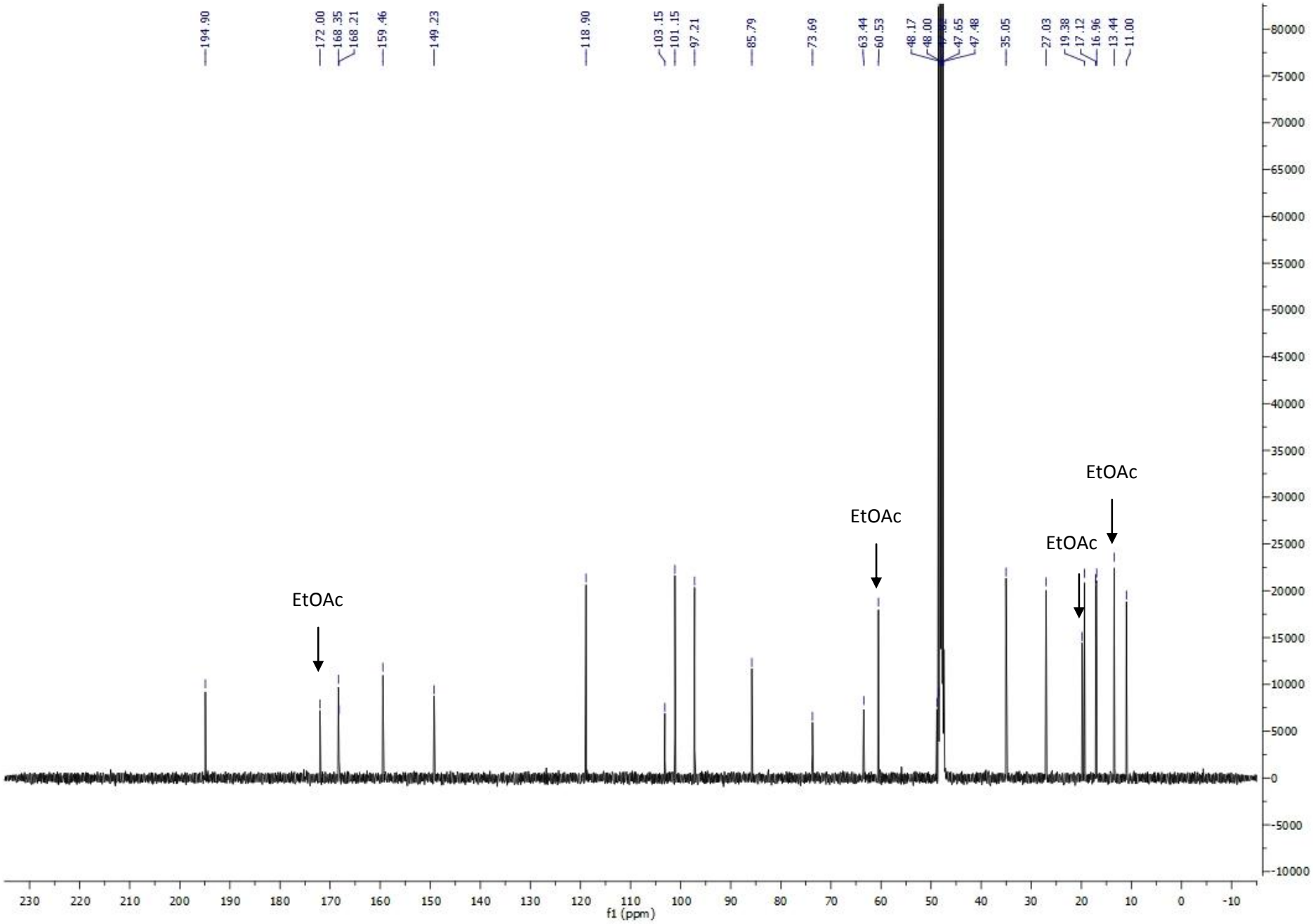

Figure S2. ^{13}C NMR (125 MHz, CD_3OD) spectrum of colletotrichone A (**1**)

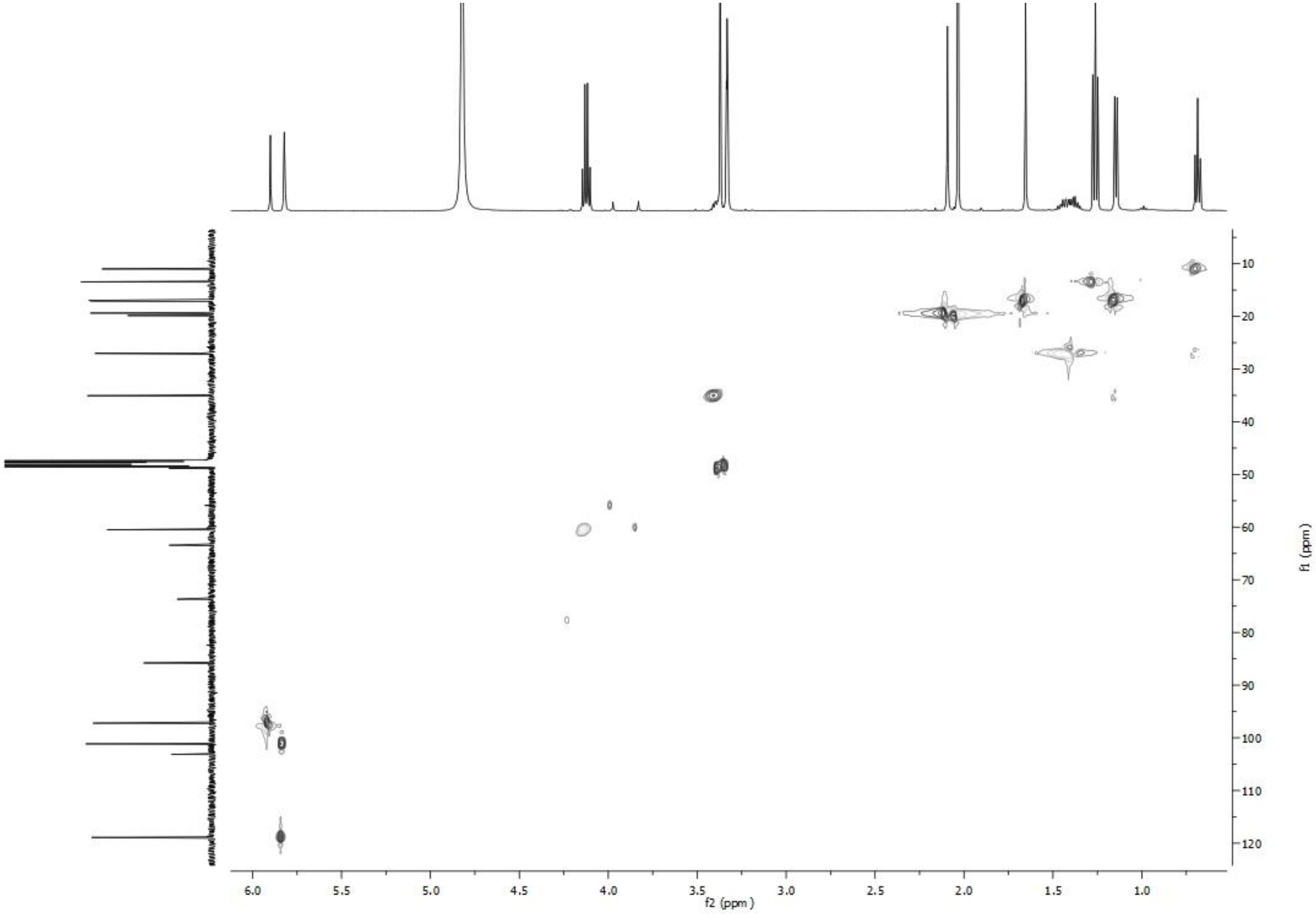

Figure S3. HSQC (500 MHz, CD_3OD) spectrum of colletotrichone A (**1**)

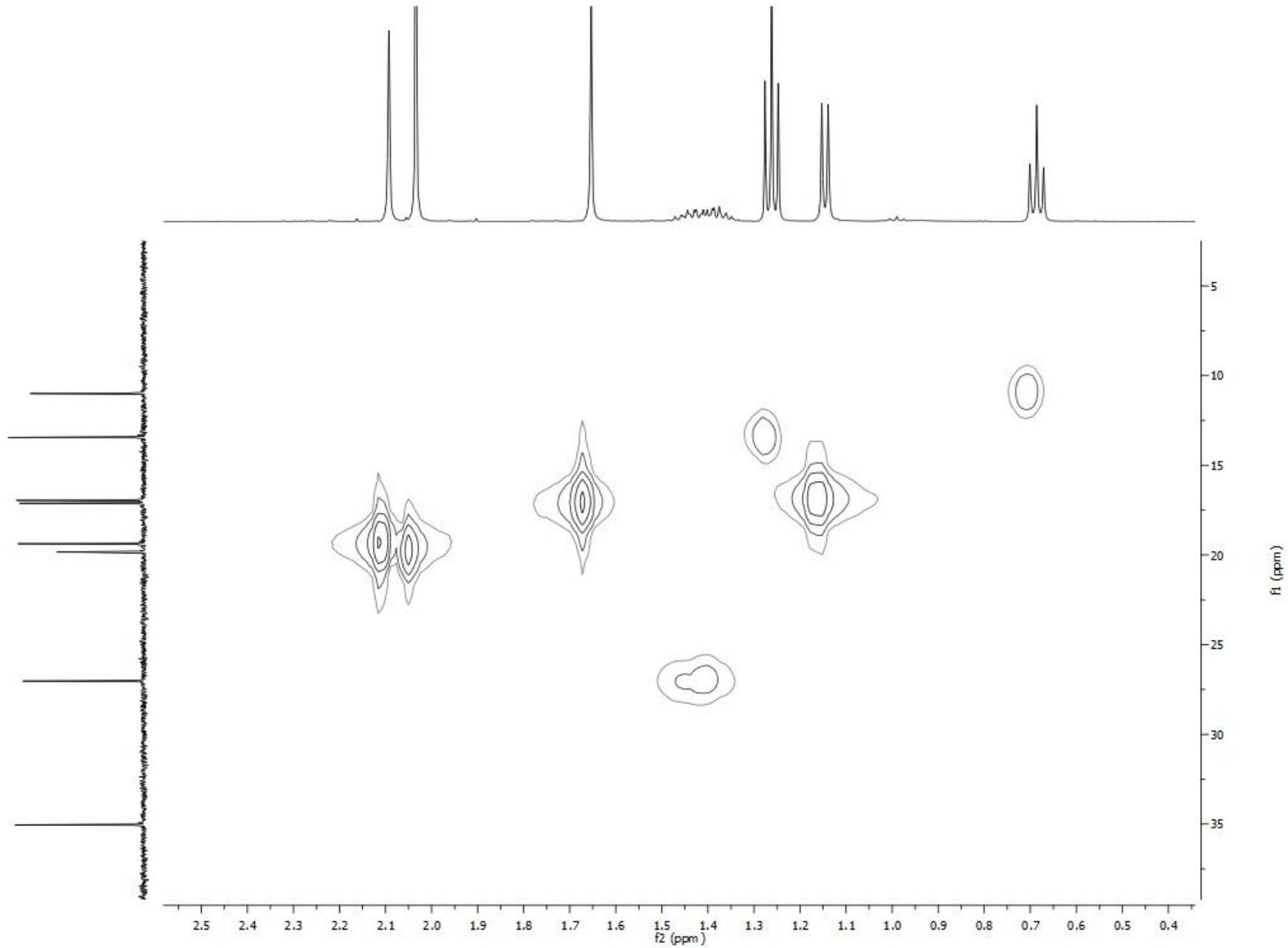

Figure S3. HSQC (500 MHz, CD_3OD) spectrum of colletotrichone A (**1**)

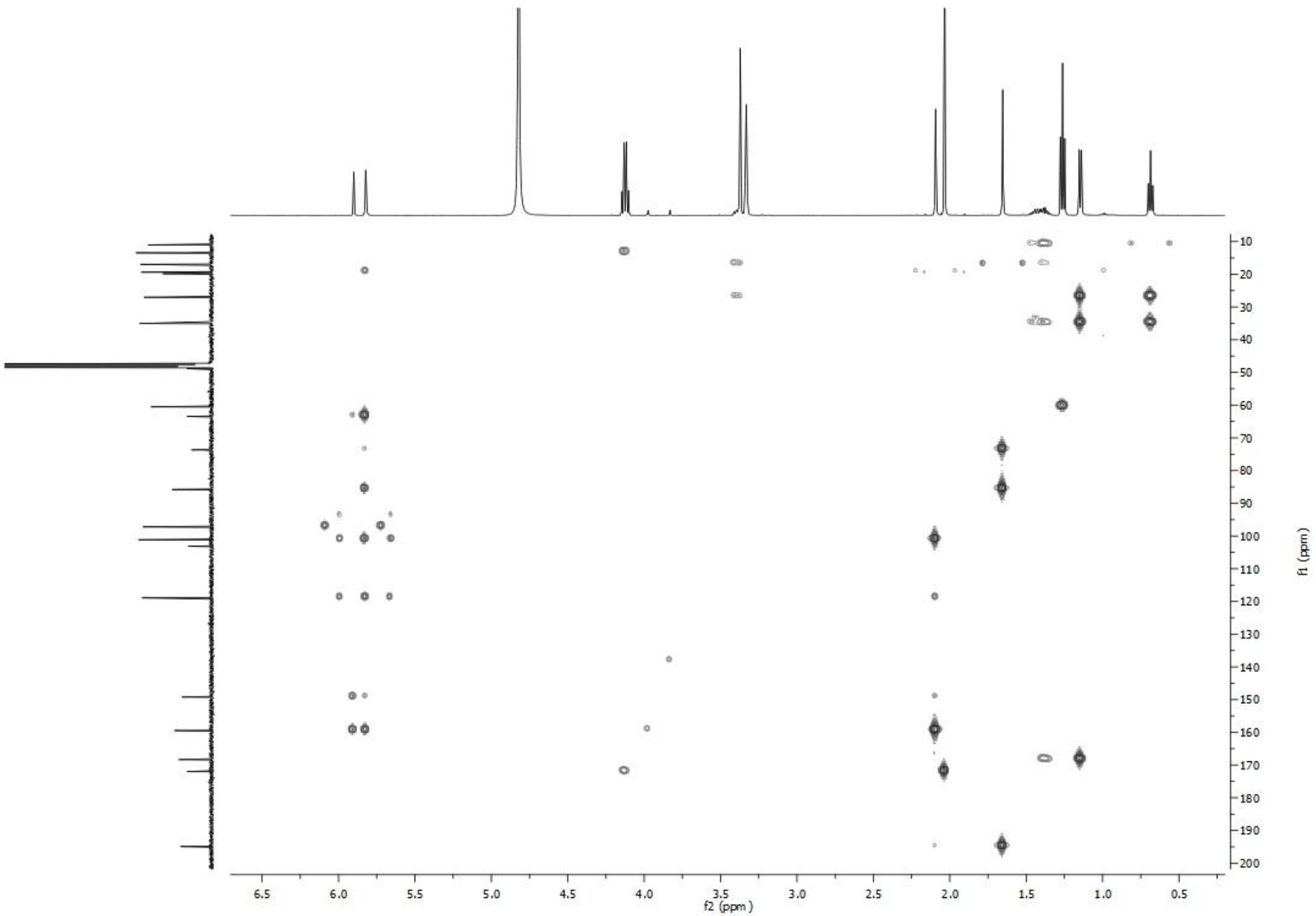

Figure S4. HMBC (500 MHz, CD_3OD) spectrum of colletotrichone A (**1**)

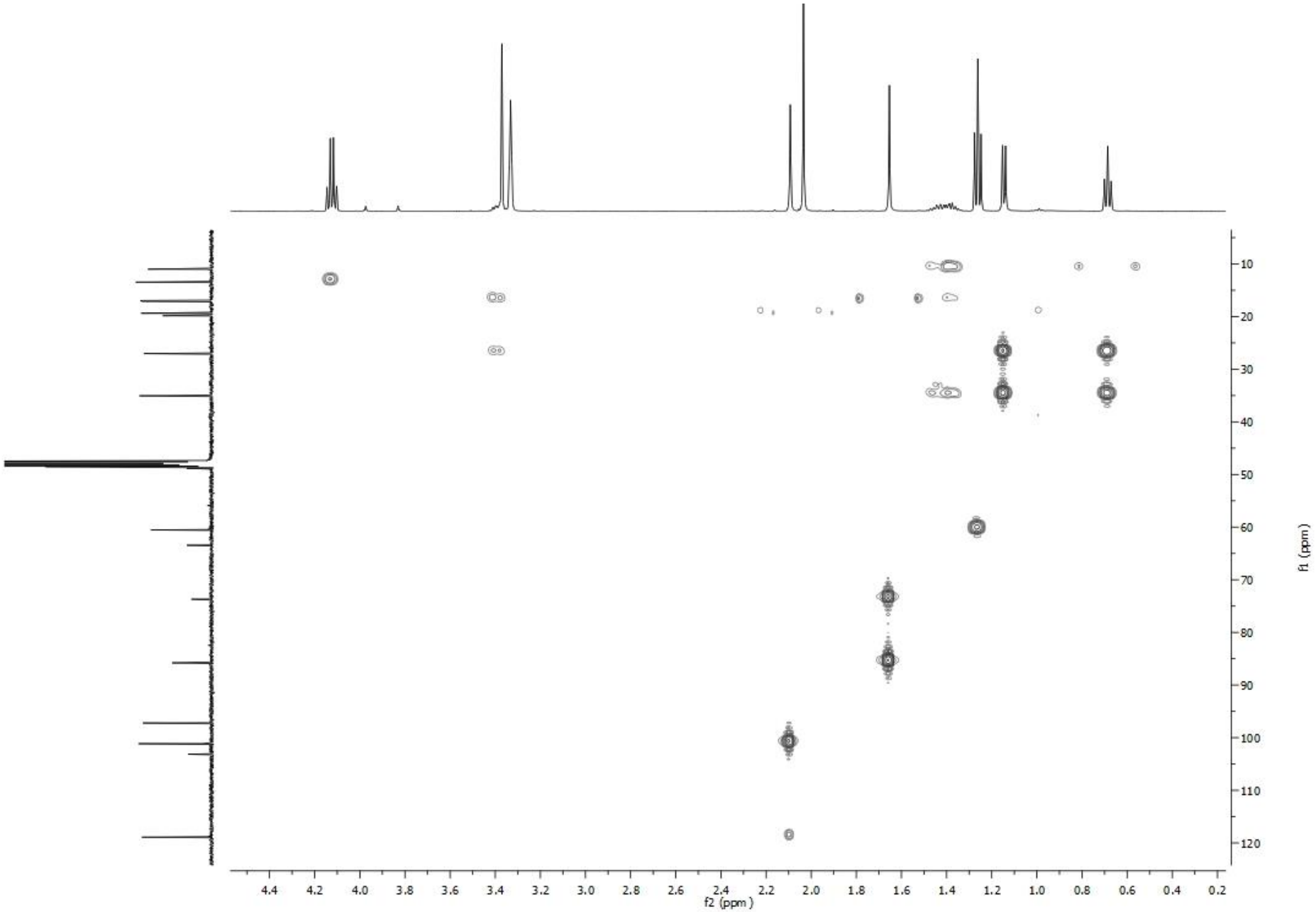

Figure S4. HMBC (500 MHz, CD_3OD) spectrum of colletotrichone A (**1**)

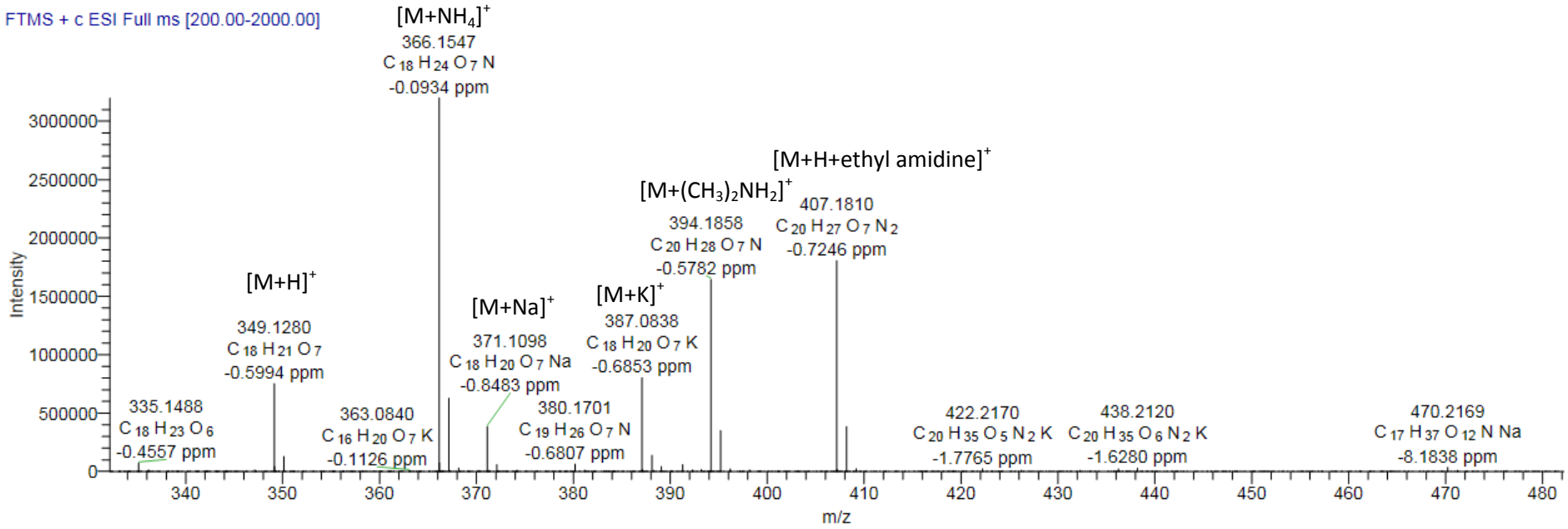

Figure S5. Positive ESIHRMS of colletotrichone A (**1**)

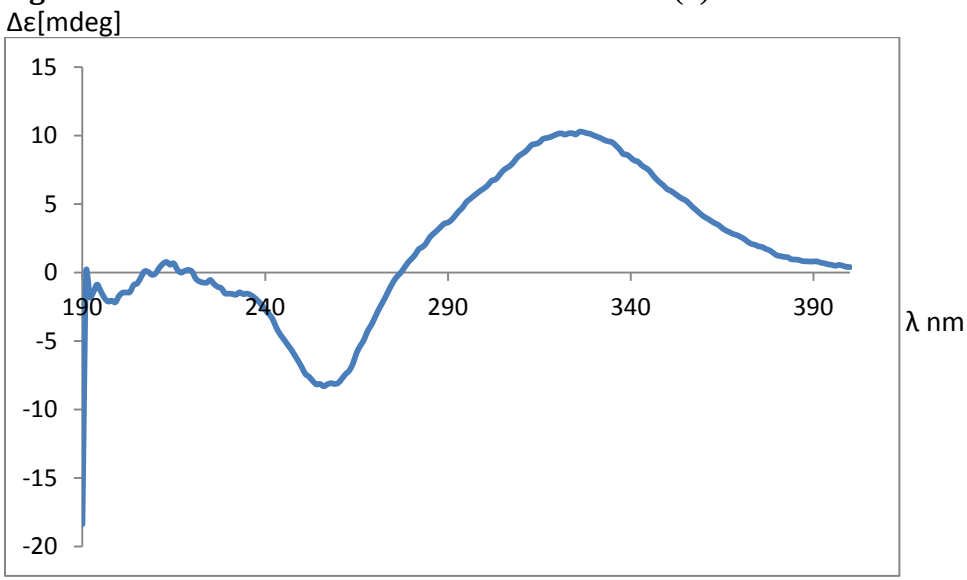

Figure S6. CD spectrum of colletotrichone A (**1**) (0.1 mg/mL, MeOH)

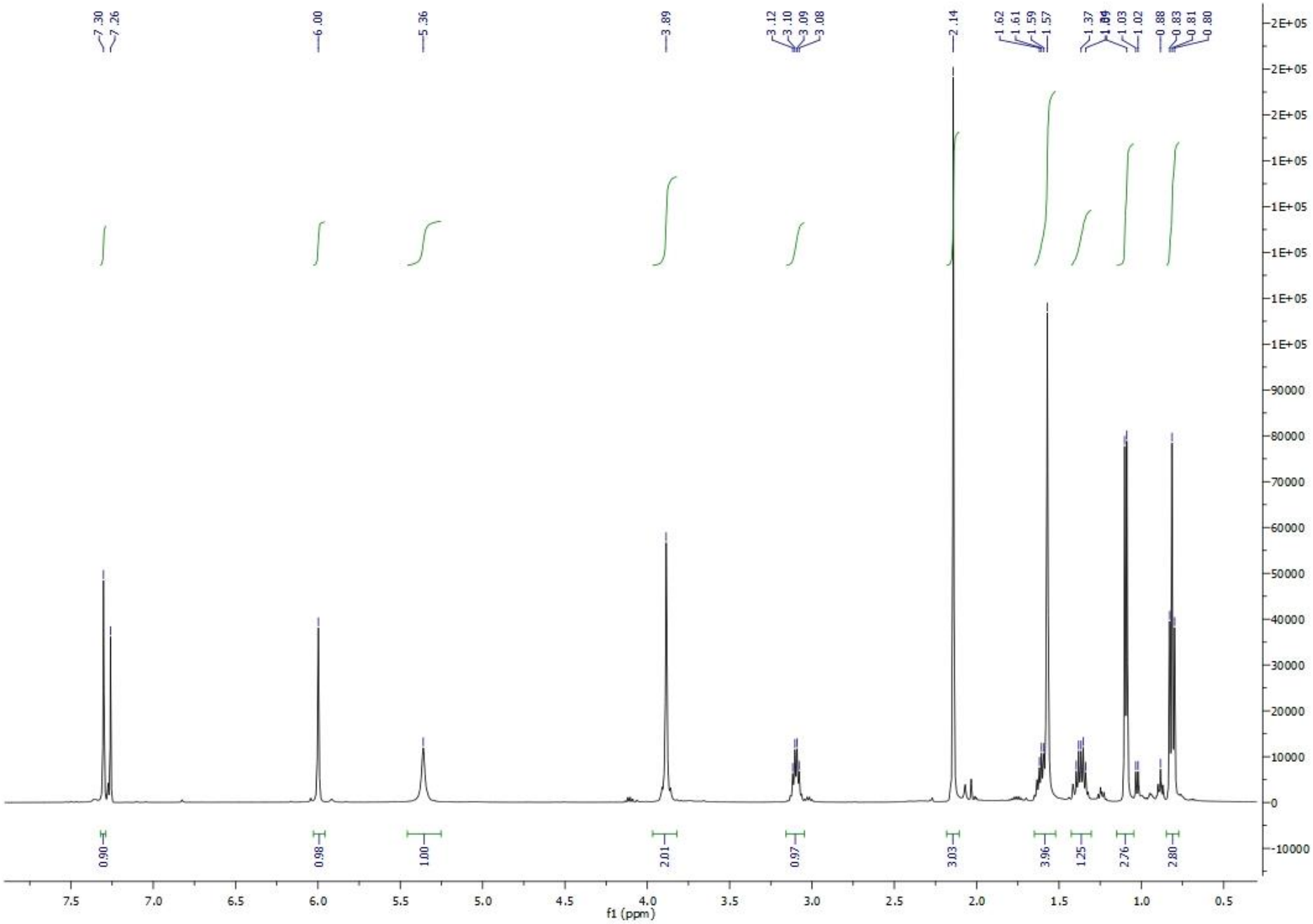

Figure S7. ^{1}H NMR (500 MHz, $CDCl_3$) spectrum of colletotrichone B (**2a**)

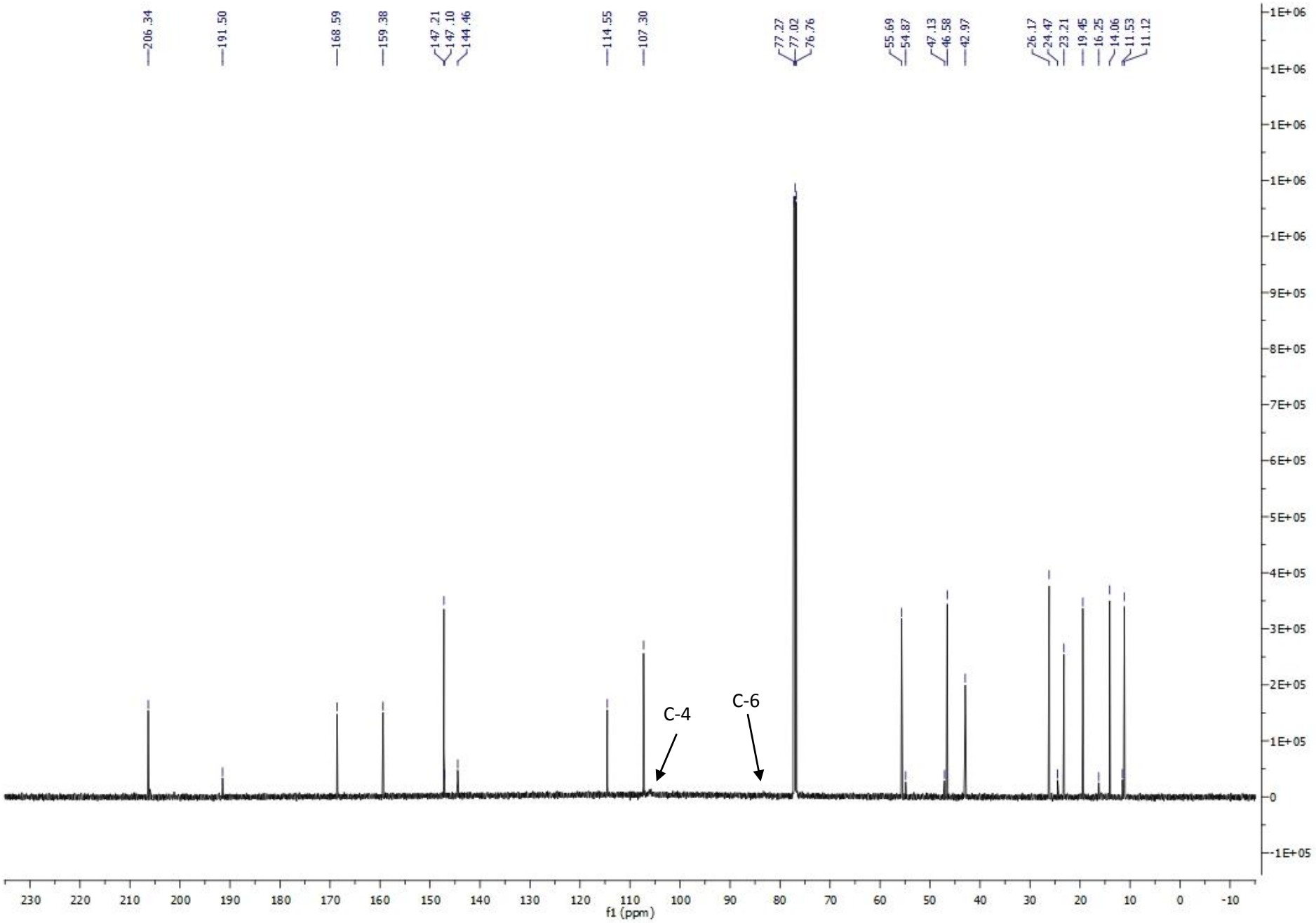

Figure S8. ^{13}C NMR (125 MHz, $CDCl_3$) spectrum of colletotrichone B (**2a**)

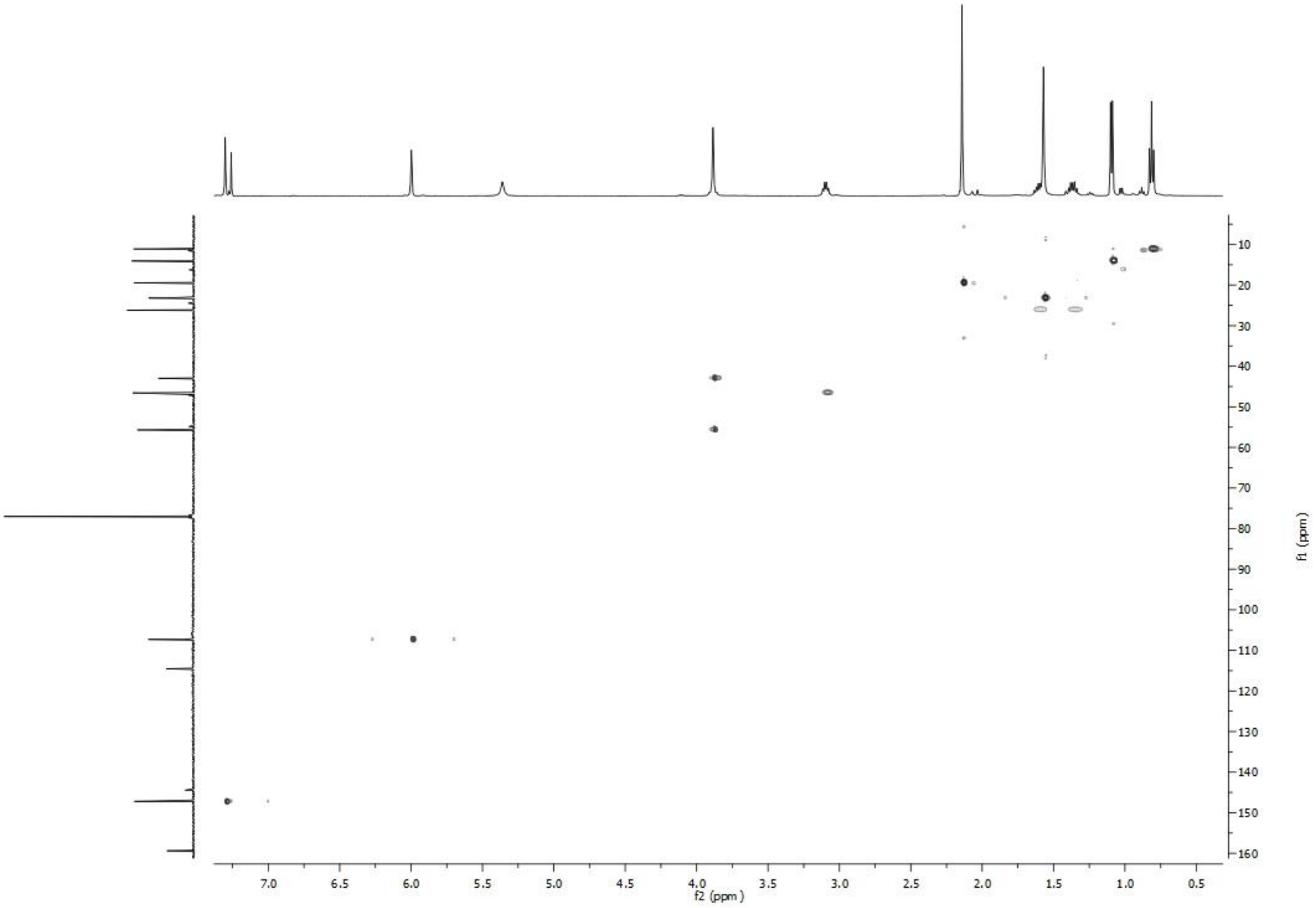

Figure S9. HSQC (500 MHz, $CDCl_3$) spectrum of colletotrichone B (**2a**)

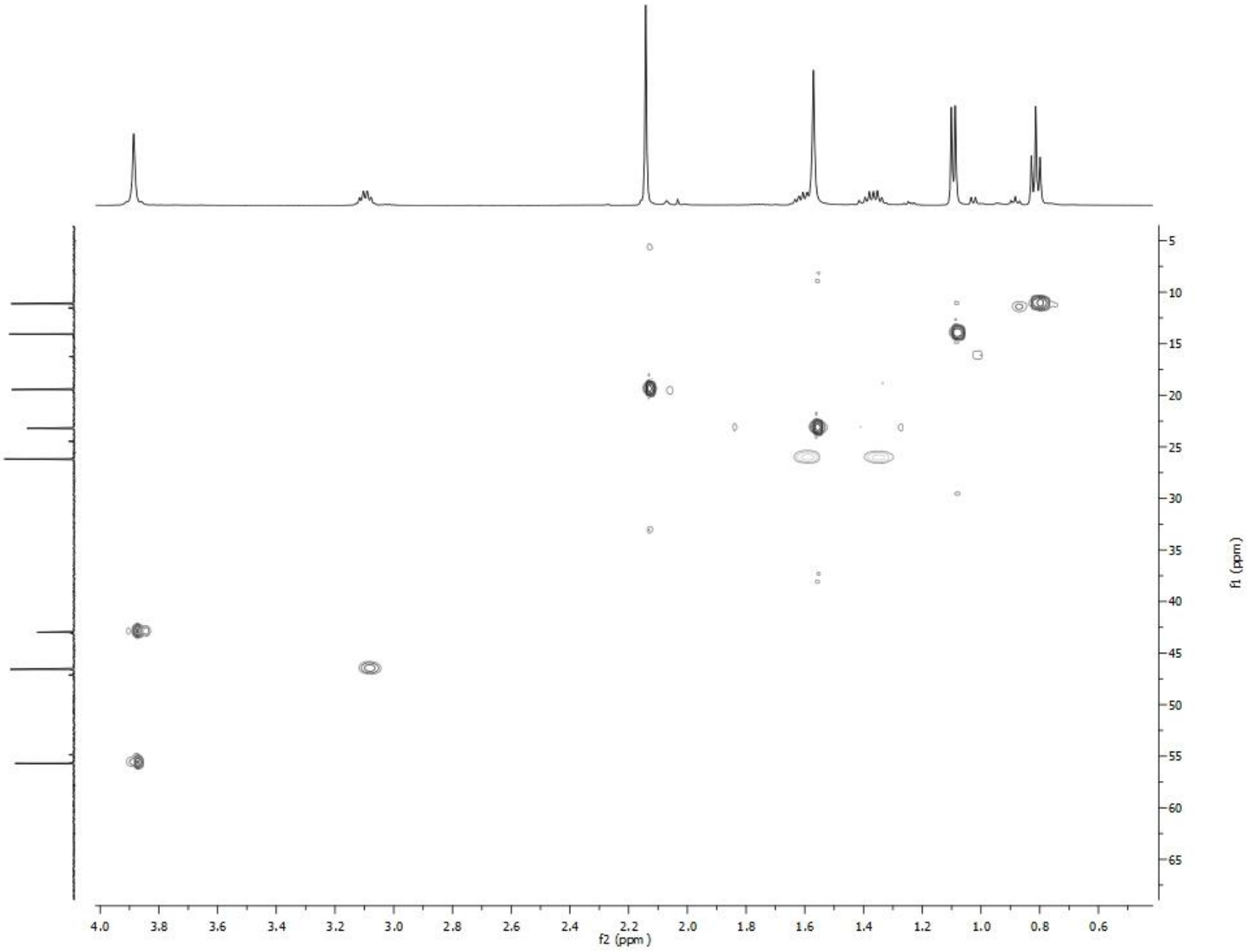

Figure S9. HSQC (500 MHz, $CDCl_3$) spectrum of colletotrichone B (**2a**)

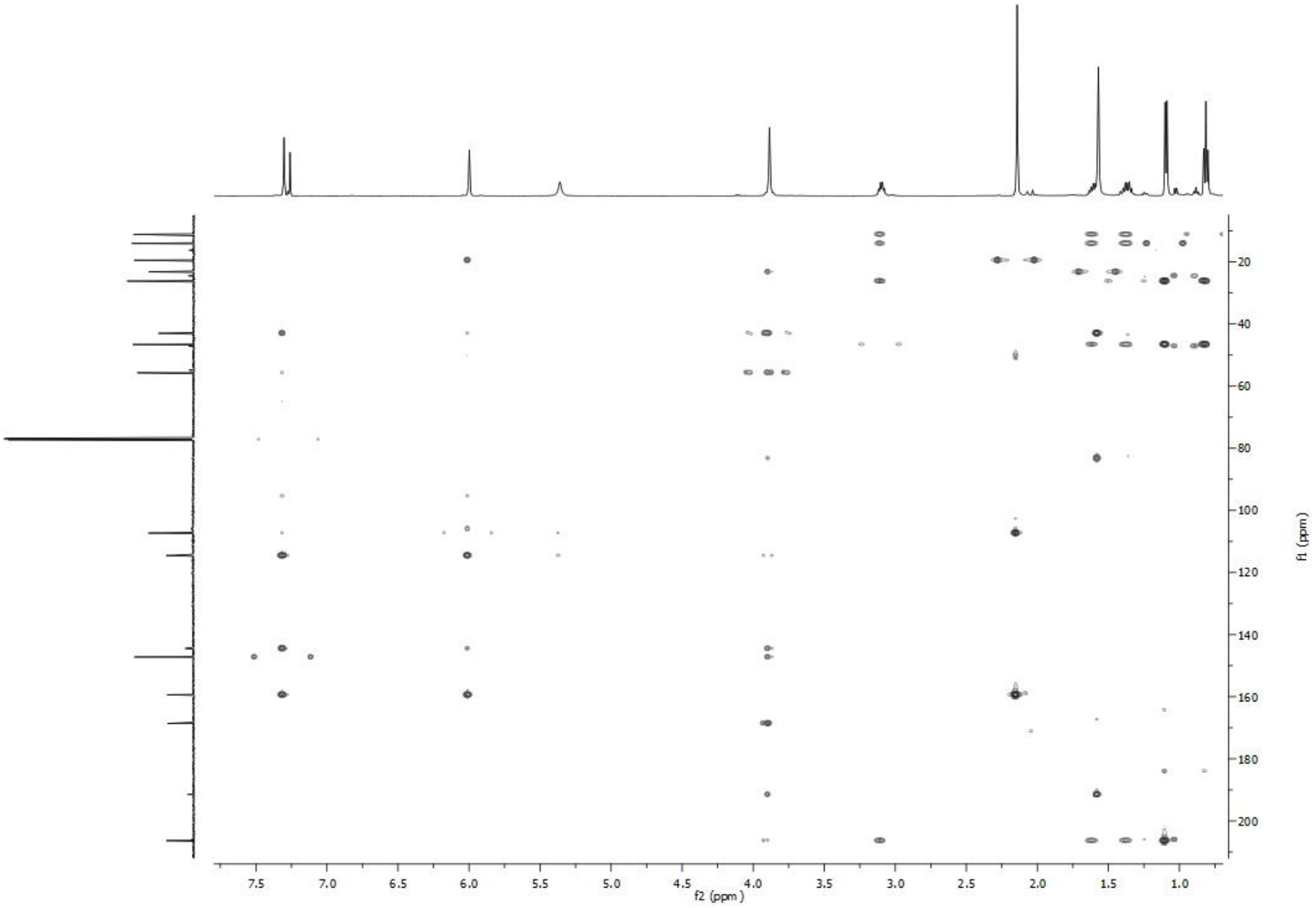

Figure S10. HMBC (500 MHz, $CDCl_3$) spectrum of colletotrichone B (**2a**)

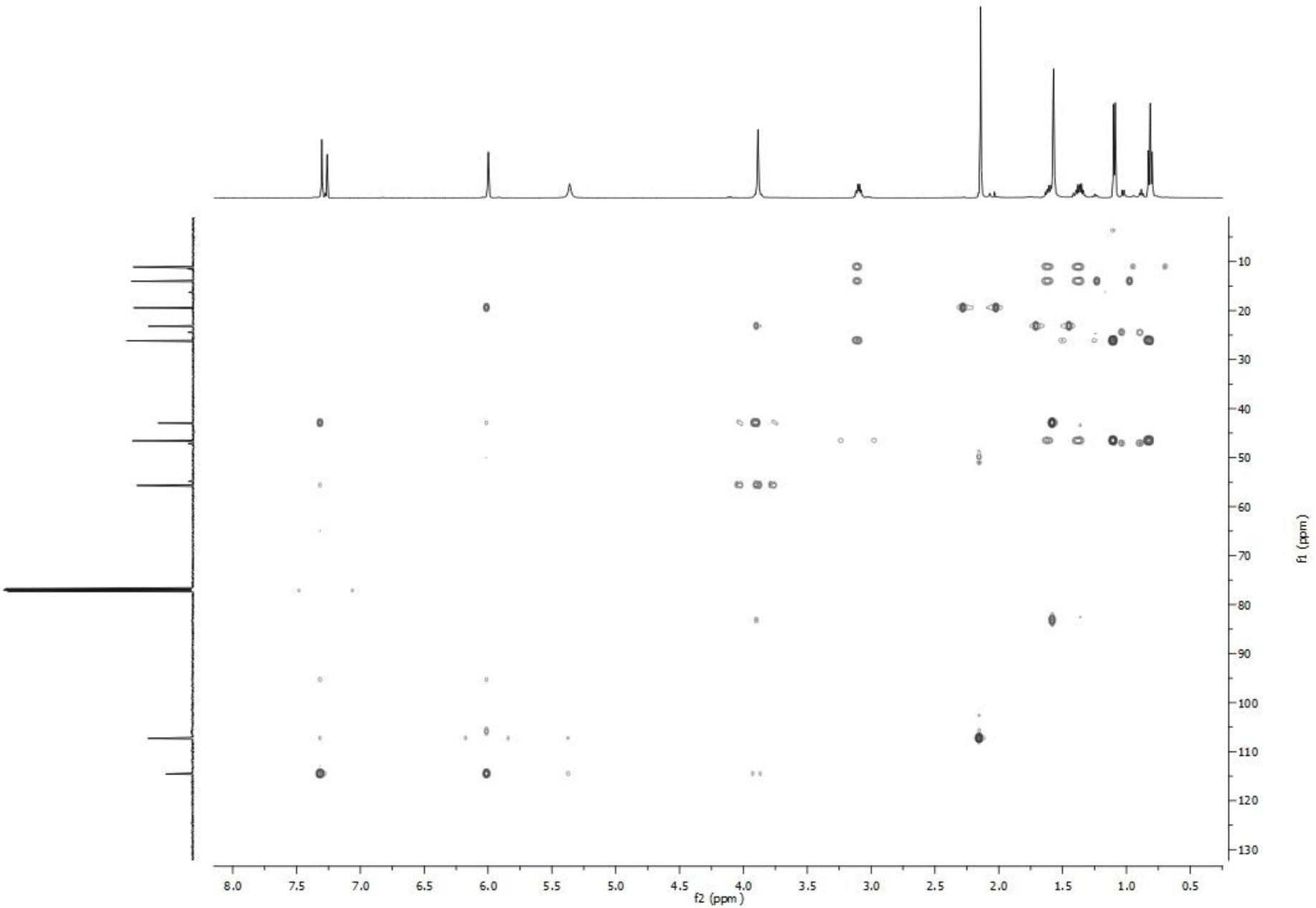

Figure S10. HMBC (500 MHz, $CDCl_3$) spectrum of colletotrichone B (**2a**)

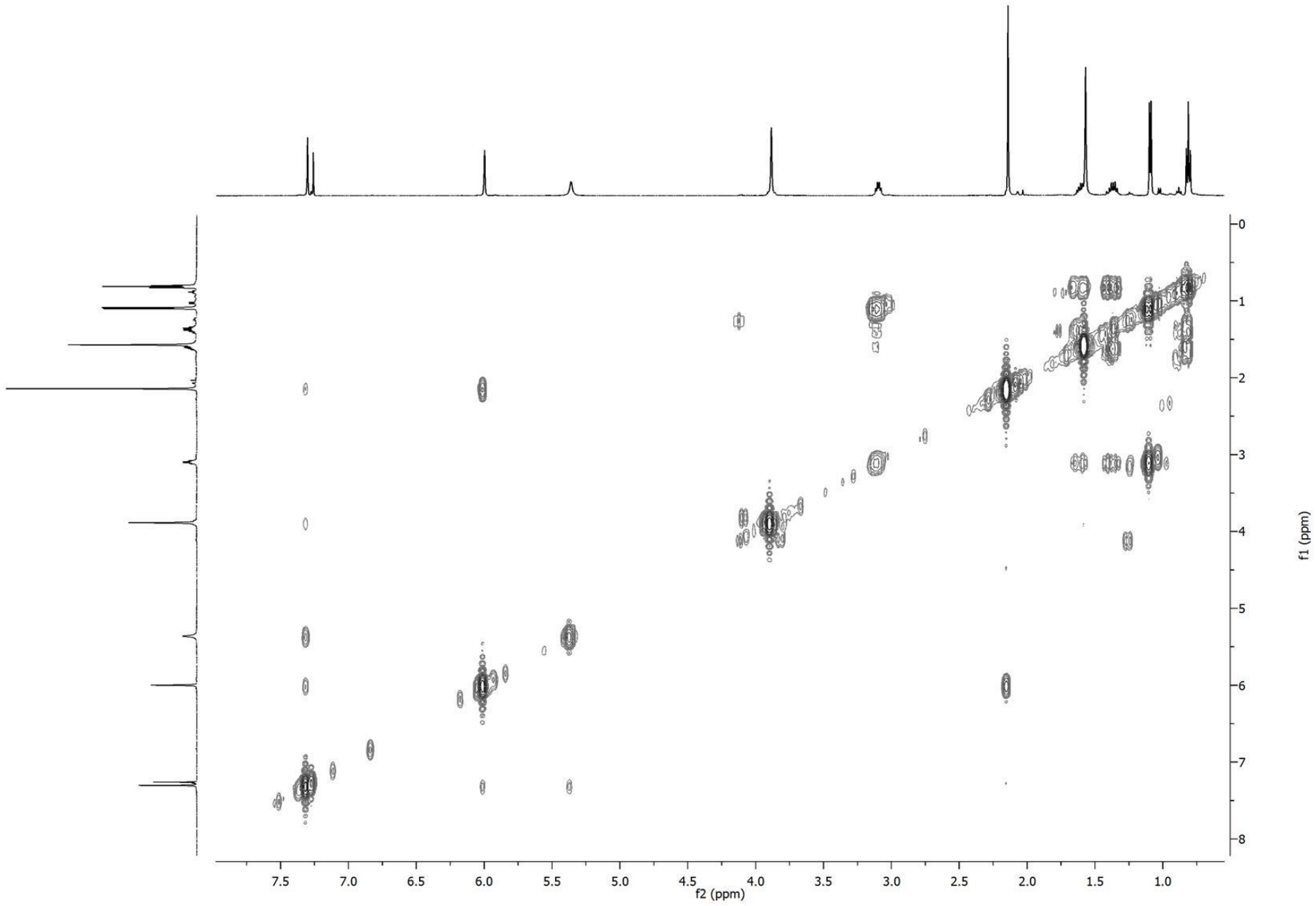

Figure S11. ^{1}H, ^{1}H COSY (500 MHz, $CDCl_3$) spectrum of colletotrichone B (**2a**)

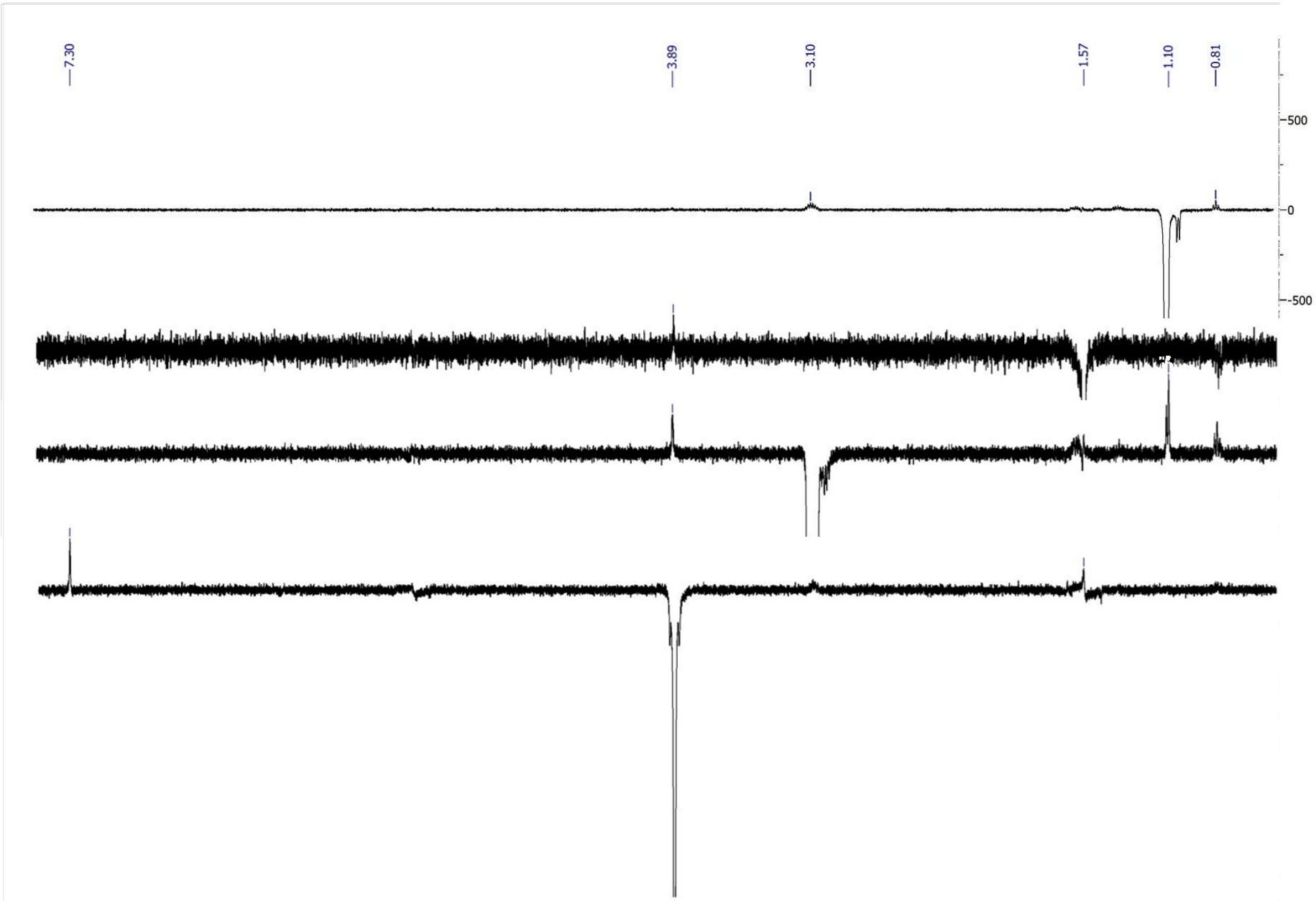

Figure S12. 1D NOESY (500 MHz, $CDCl_3$) spectrum of colletotrichone B (**2a**)

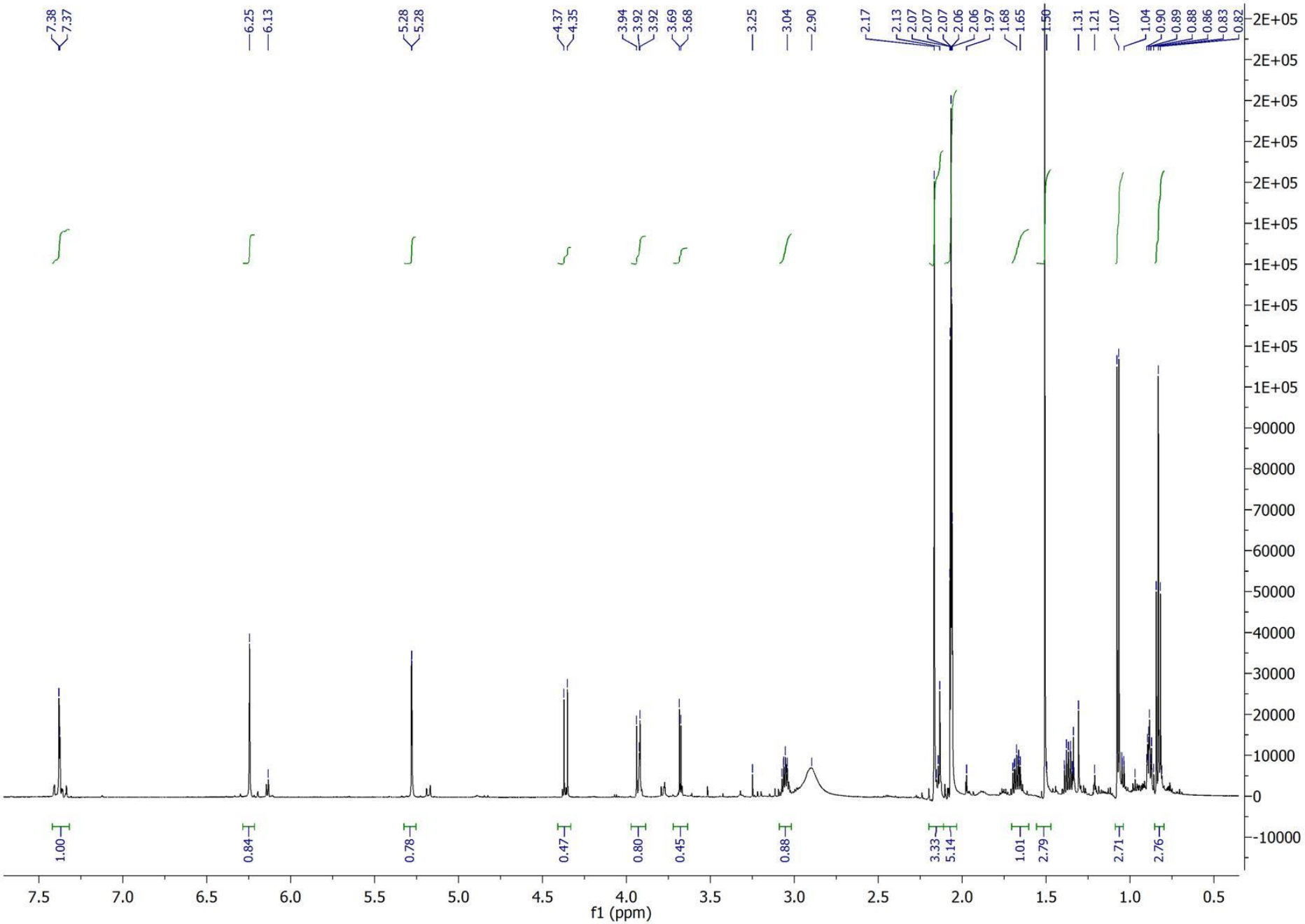

Figure S13. ^{1}H NMR (500 MHz, acetone-d_6) spectrum of colletotrichone B (**2a**)

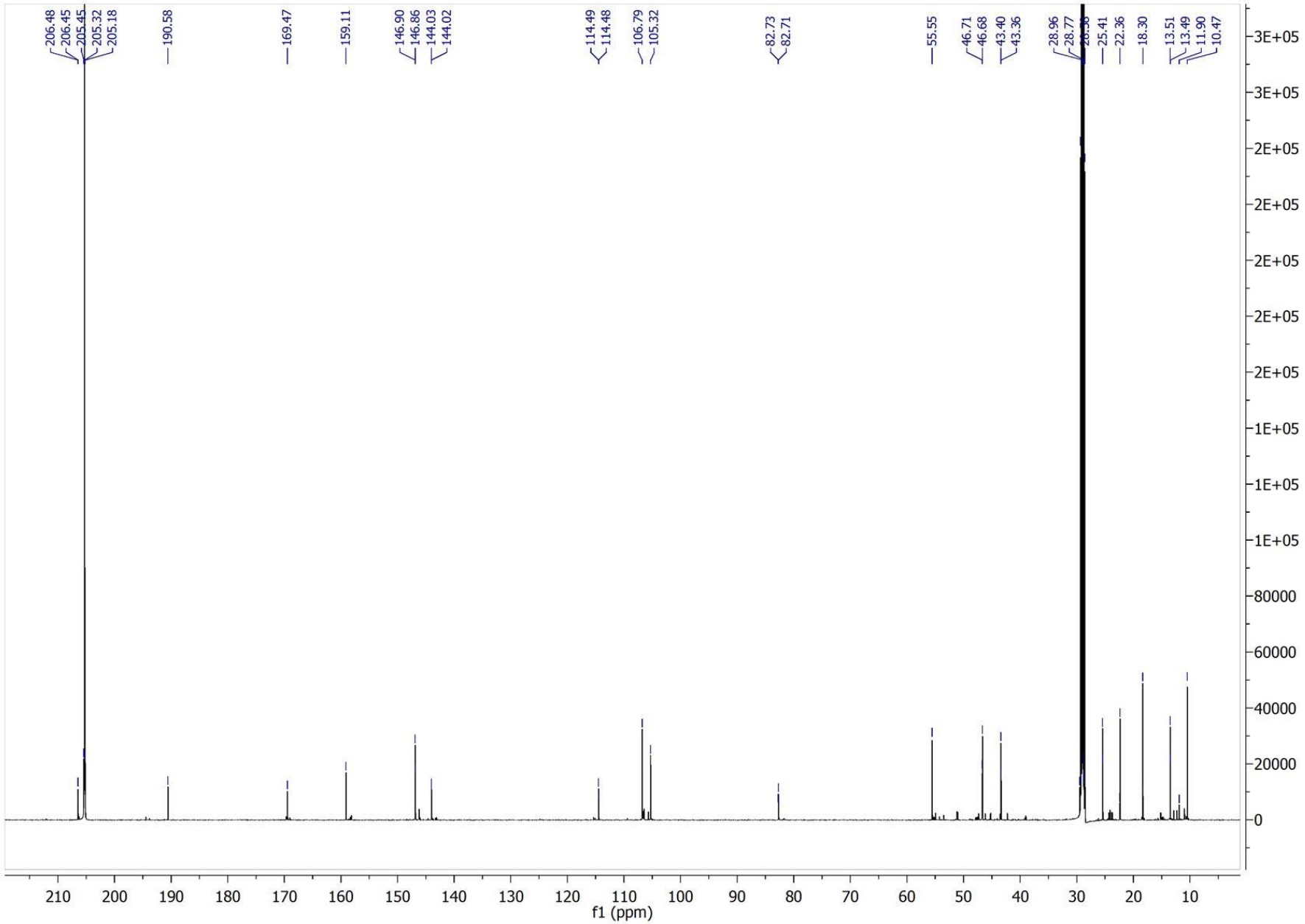

Figure S14. ^{13}C NMR (125 MHz, acetone-d_6) spectrum of colletotrichone B (**2a**)

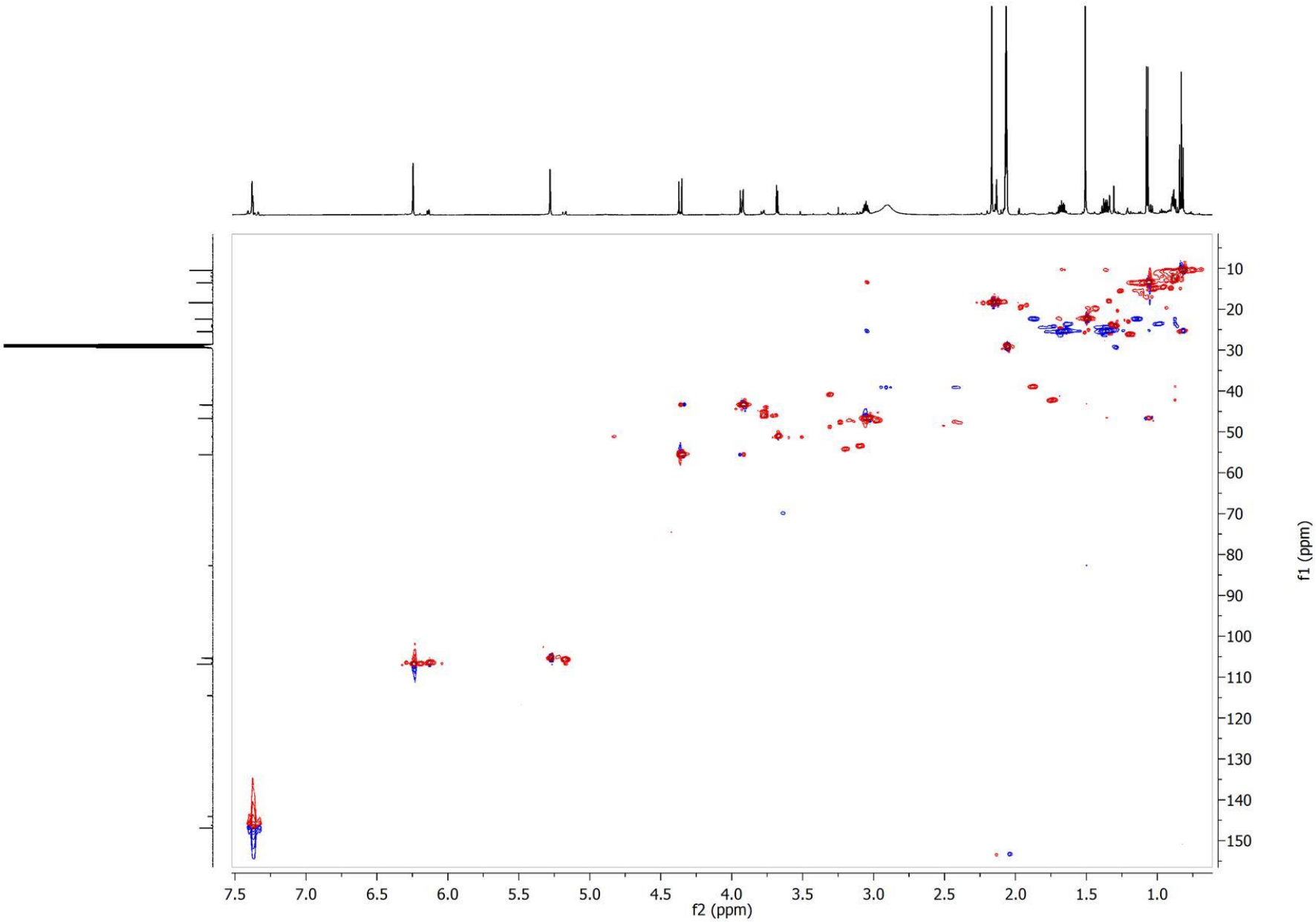

Figure S15. HSQC (500 MHz, acetone-d_6) spectrum of colletotrichone B (**2a**)

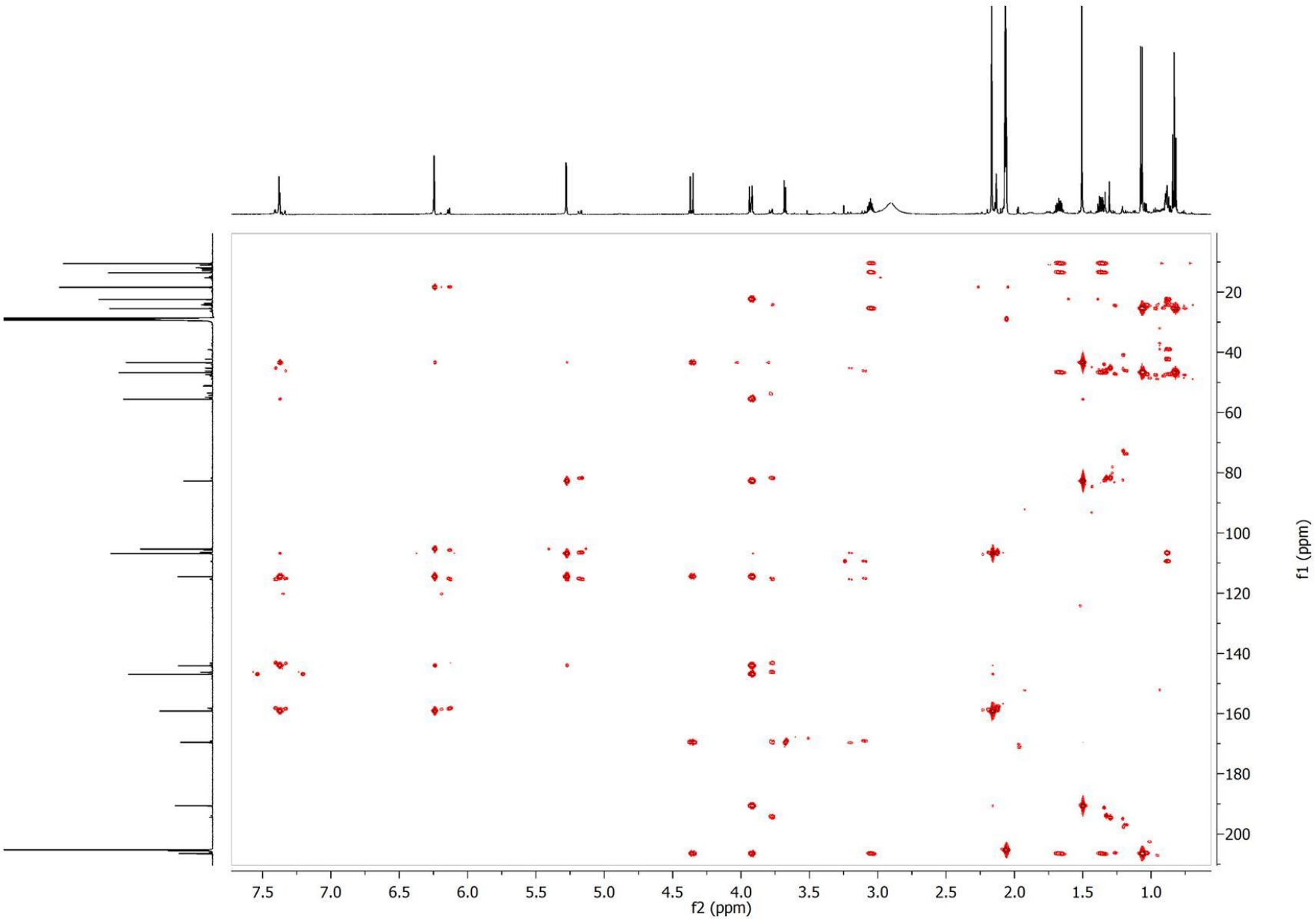

Figure S16. HMBC (500 MHz, acetone-d_6) spectrum of colletotrichone B (**2a**)

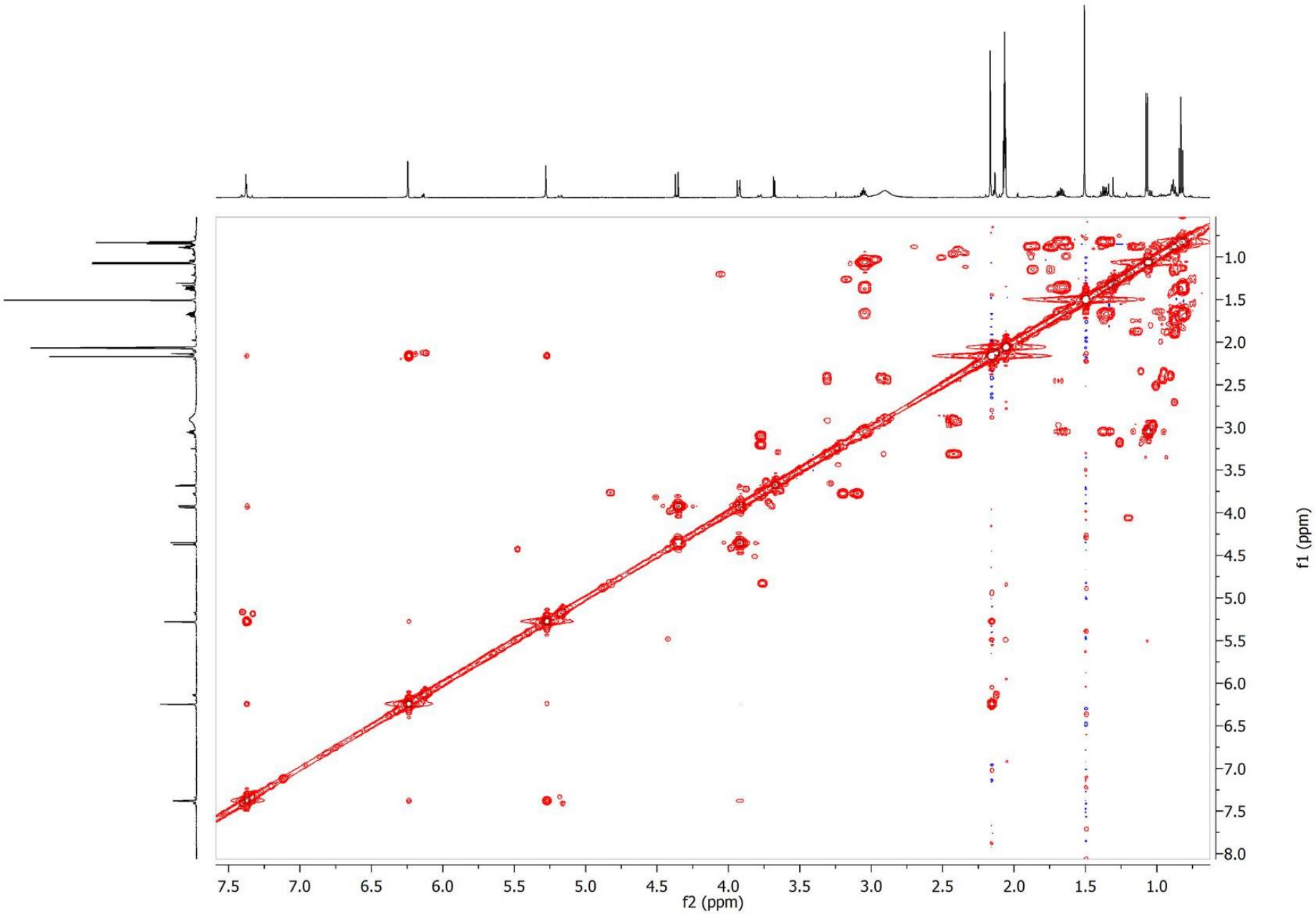

Figure S17. ^{1}H, ^{1}H COSY (500 MHz, acetone-d_6) spectrum of colletotrichone B (**2a**)

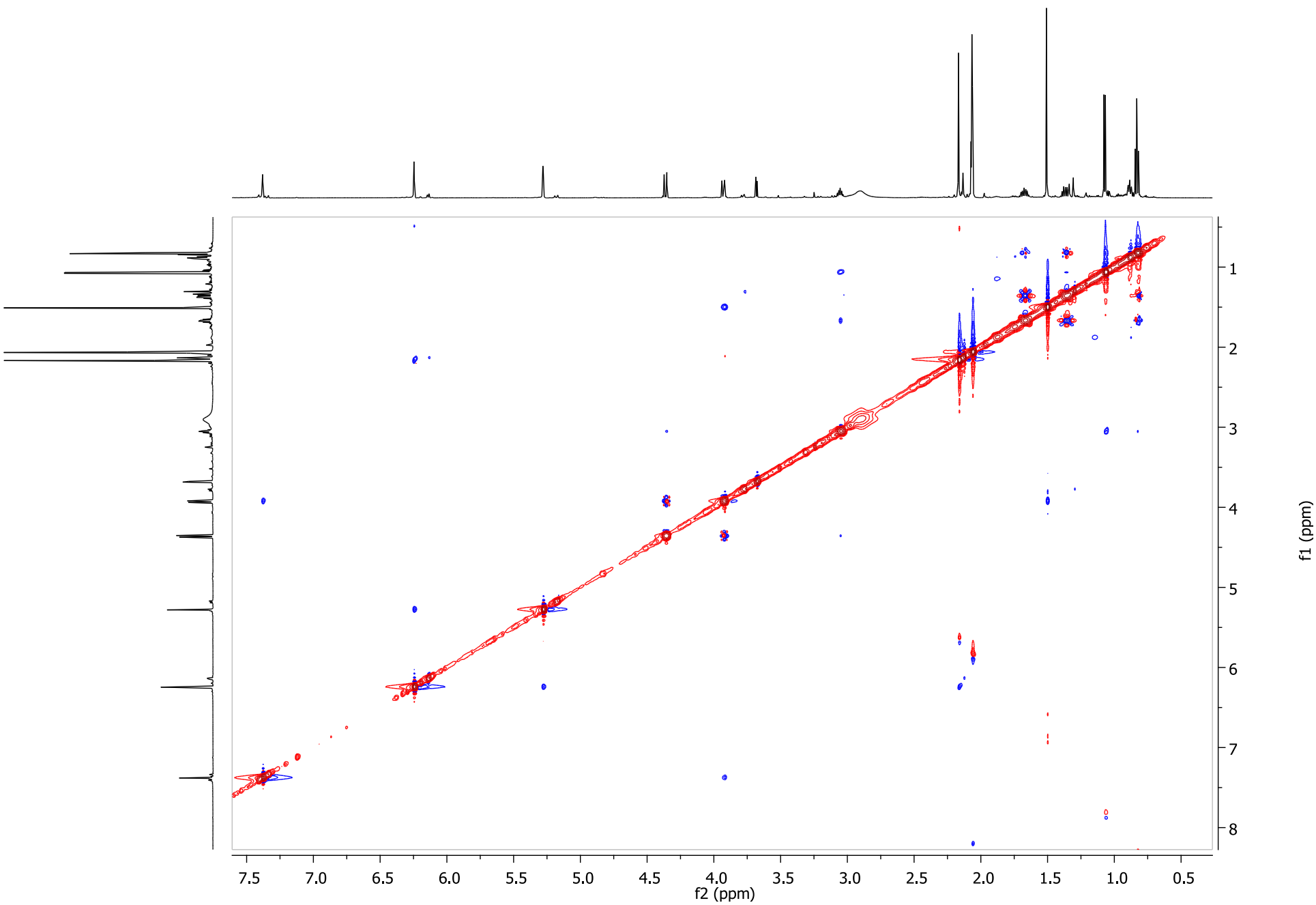

Figure S18. NOESY (500 MHz, acetone-d_6) spectrum of colletotrichone B (**2a**)

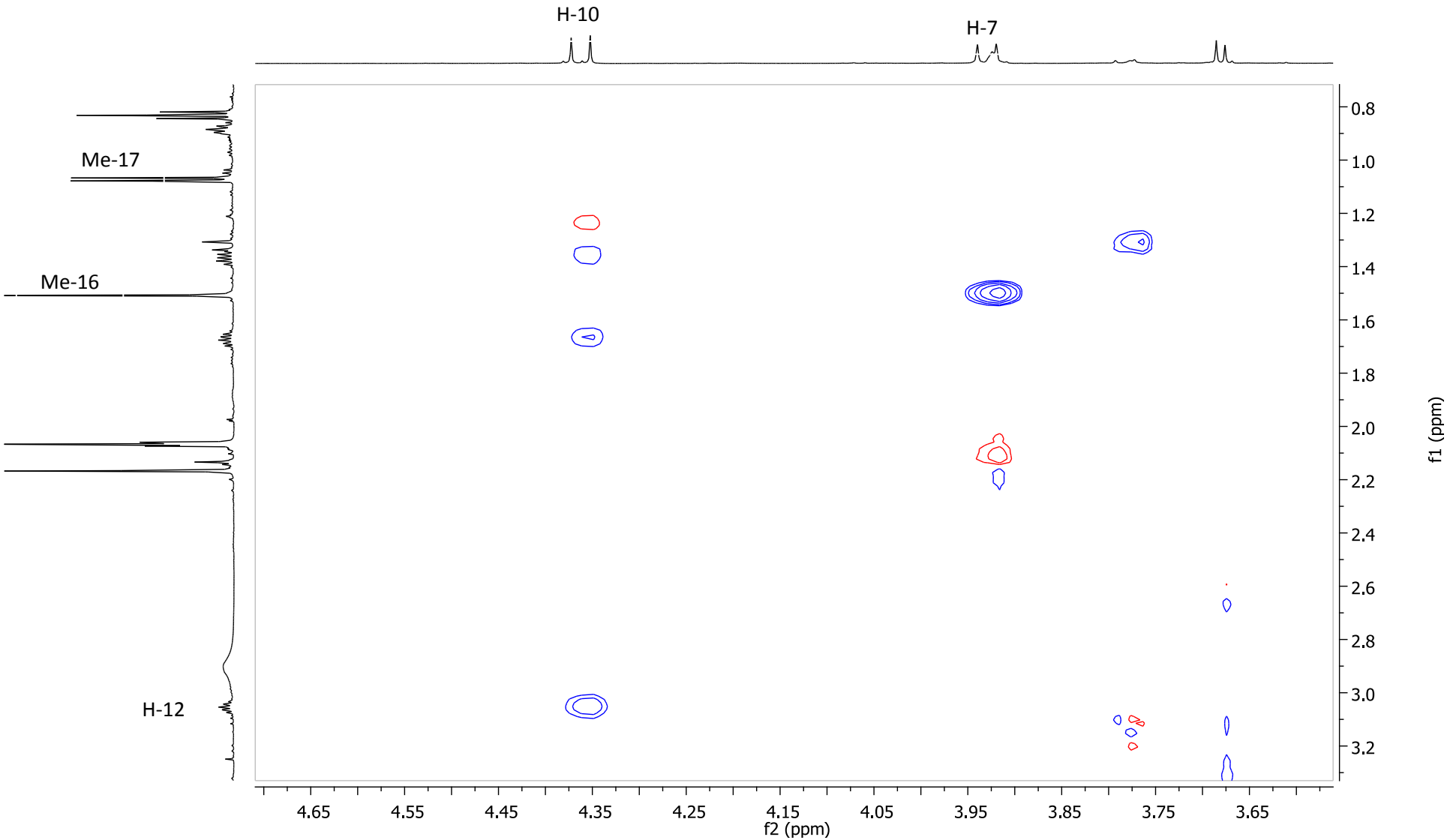

Figure S18. NOESY (500 MHz, acetone-d_6) spectrum of colletotrichone B (**2a**)

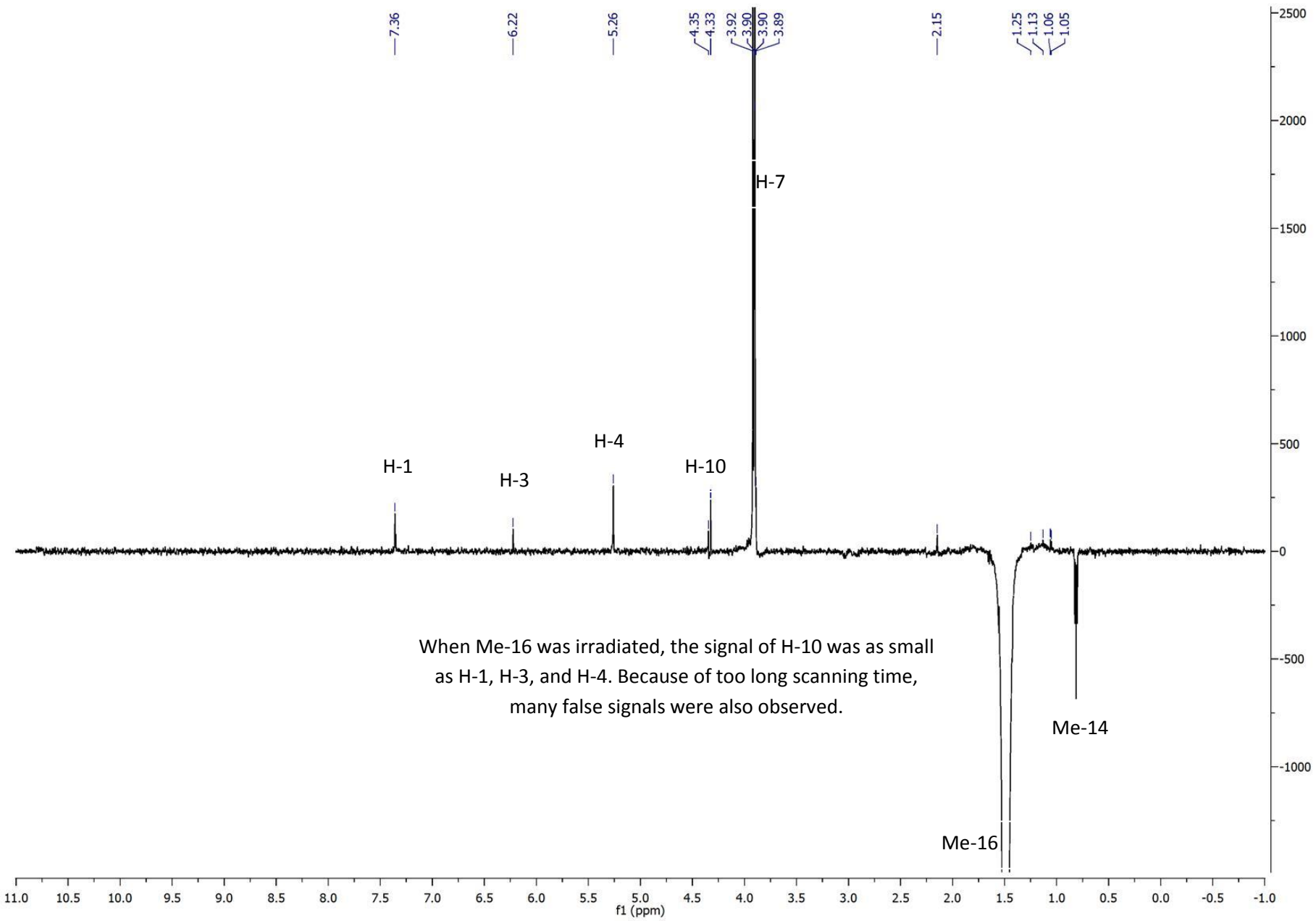

Figure S19. 1D NOESY (500 MHz, acetone-d_6) spectrum of colletotrichone B (**2a**)

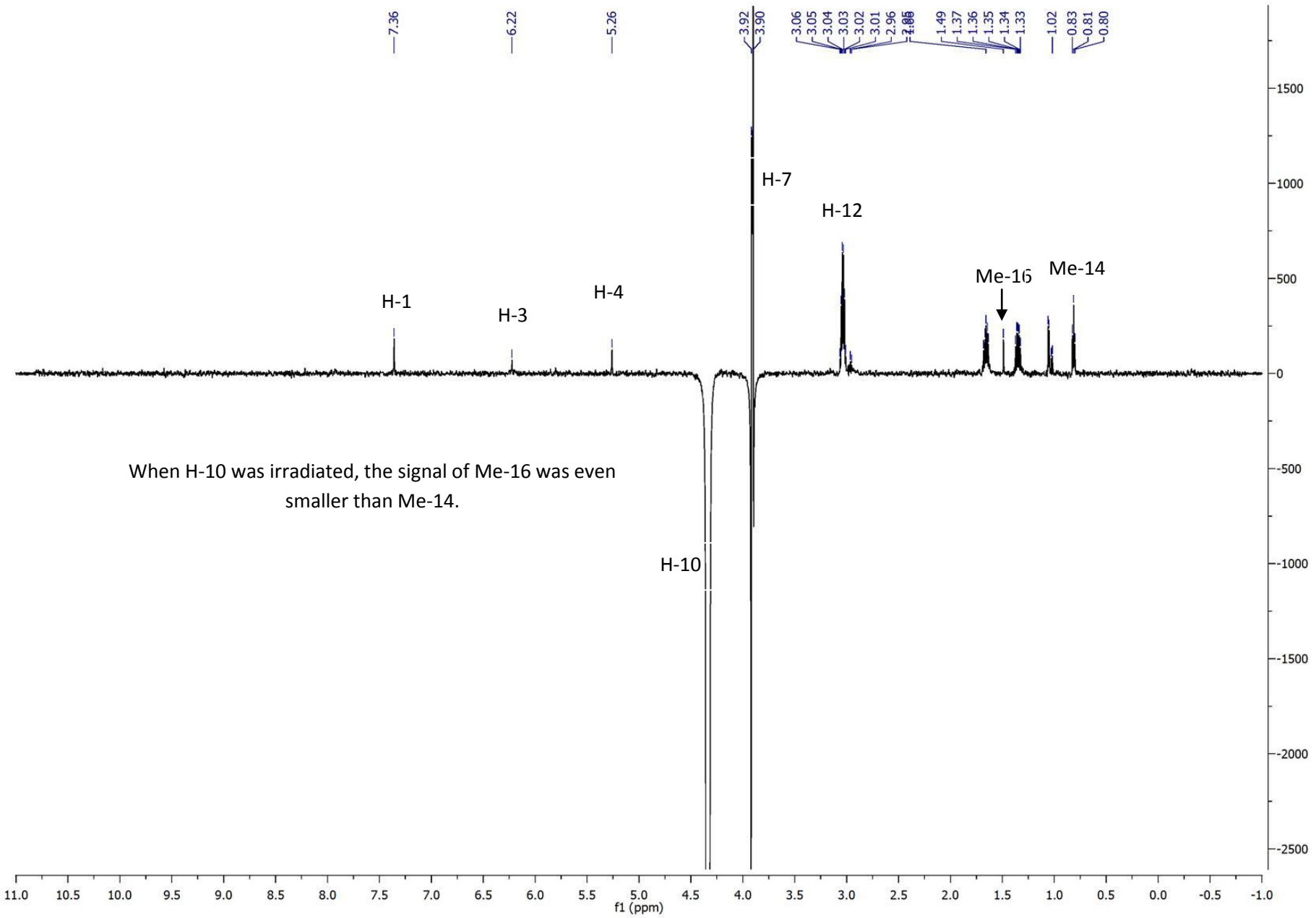

Figure S19. 1D NOESY (500 MHz, acetone-d_6) spectrum of colletotrichone B (**2a**)

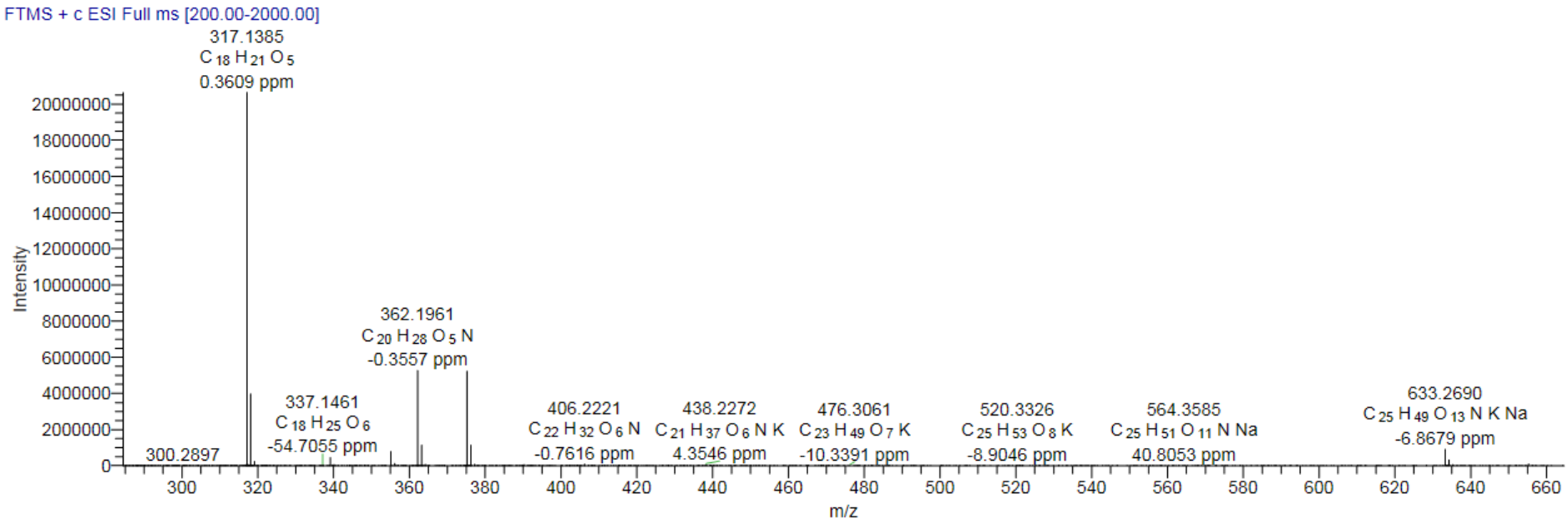

Figure S20. Positive ESIHRMS of colletotrichone B (**2a**)

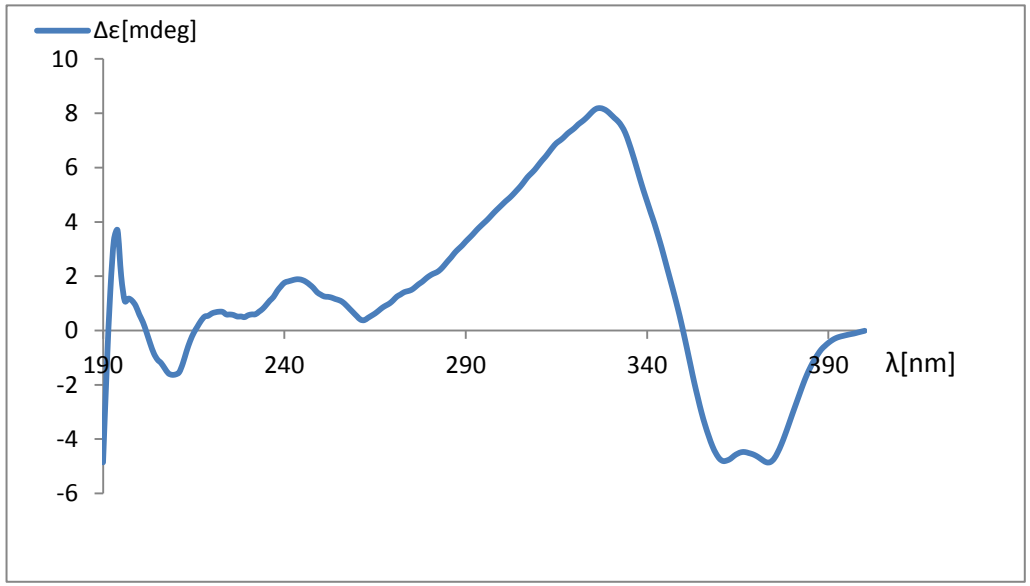

Figure S21. CD spectrum of colletotrichone B (**2a**) (0.1 mg/mL, MeOH)

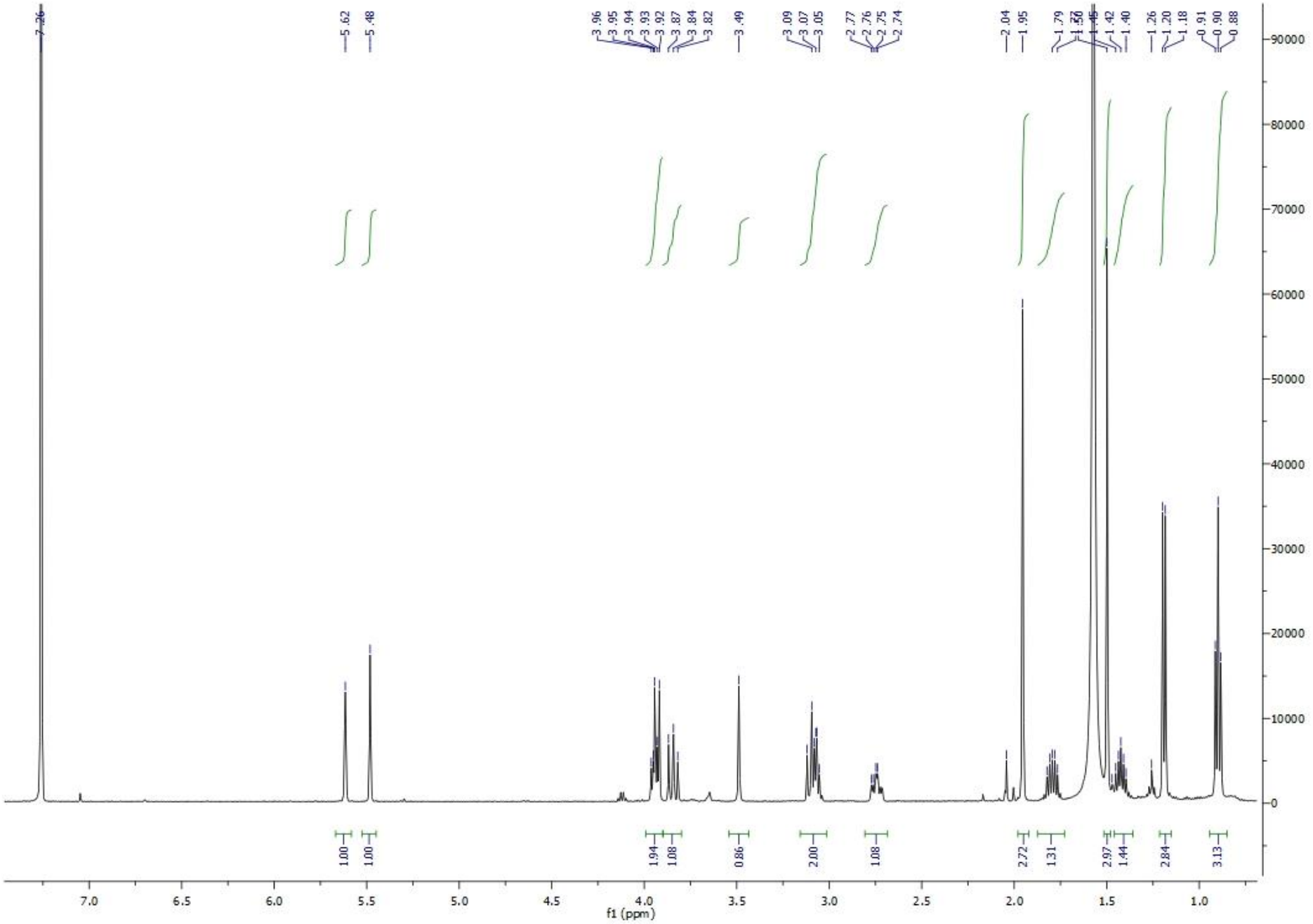

Figure S22. ^{1}H NMR (500 MHz, $CDCl_3$) spectrum of colletotrichone C (**3**)

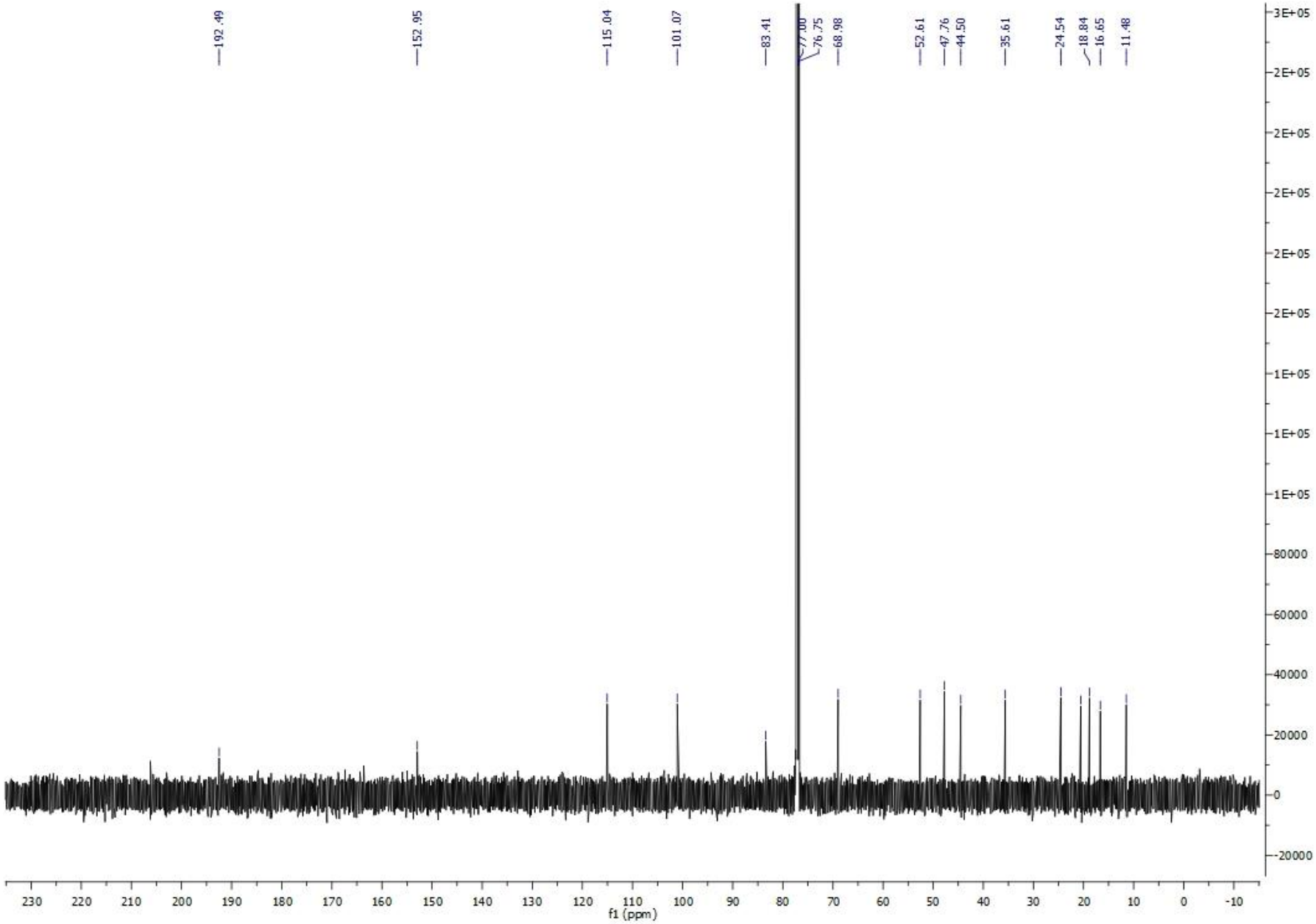

Figure S23. ^{13}C NMR (125 MHz, $CDCl_3$) spectrum of colletotrichone C (**3**)

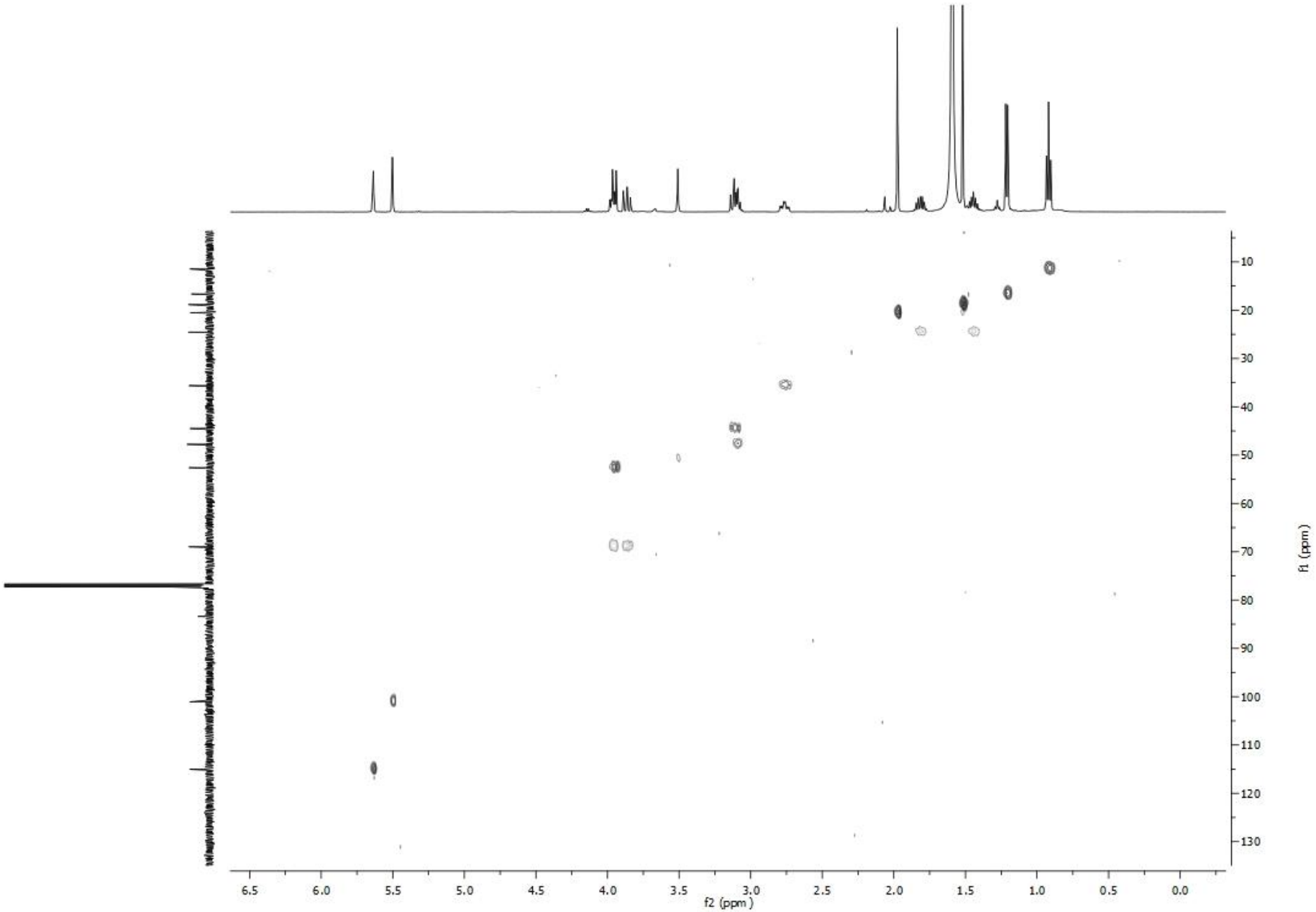

Figure S24. HSQC (500 MHz, $CDCl_3$) spectrum of colletotrichone C (**3**)

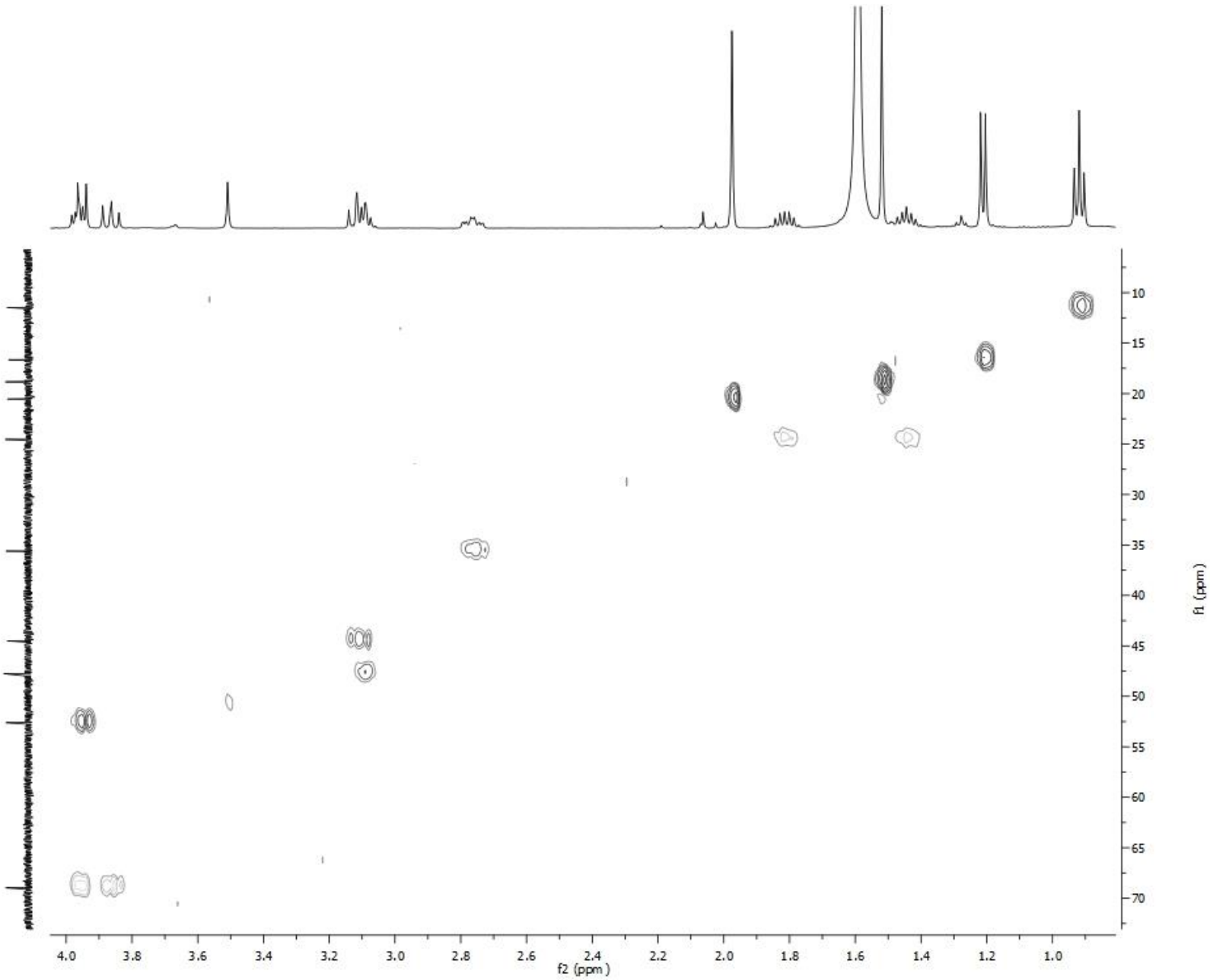

Figure S24. HSQC (500 MHz, $CDCl_3$) spectrum of colletotrichone C (**3**)

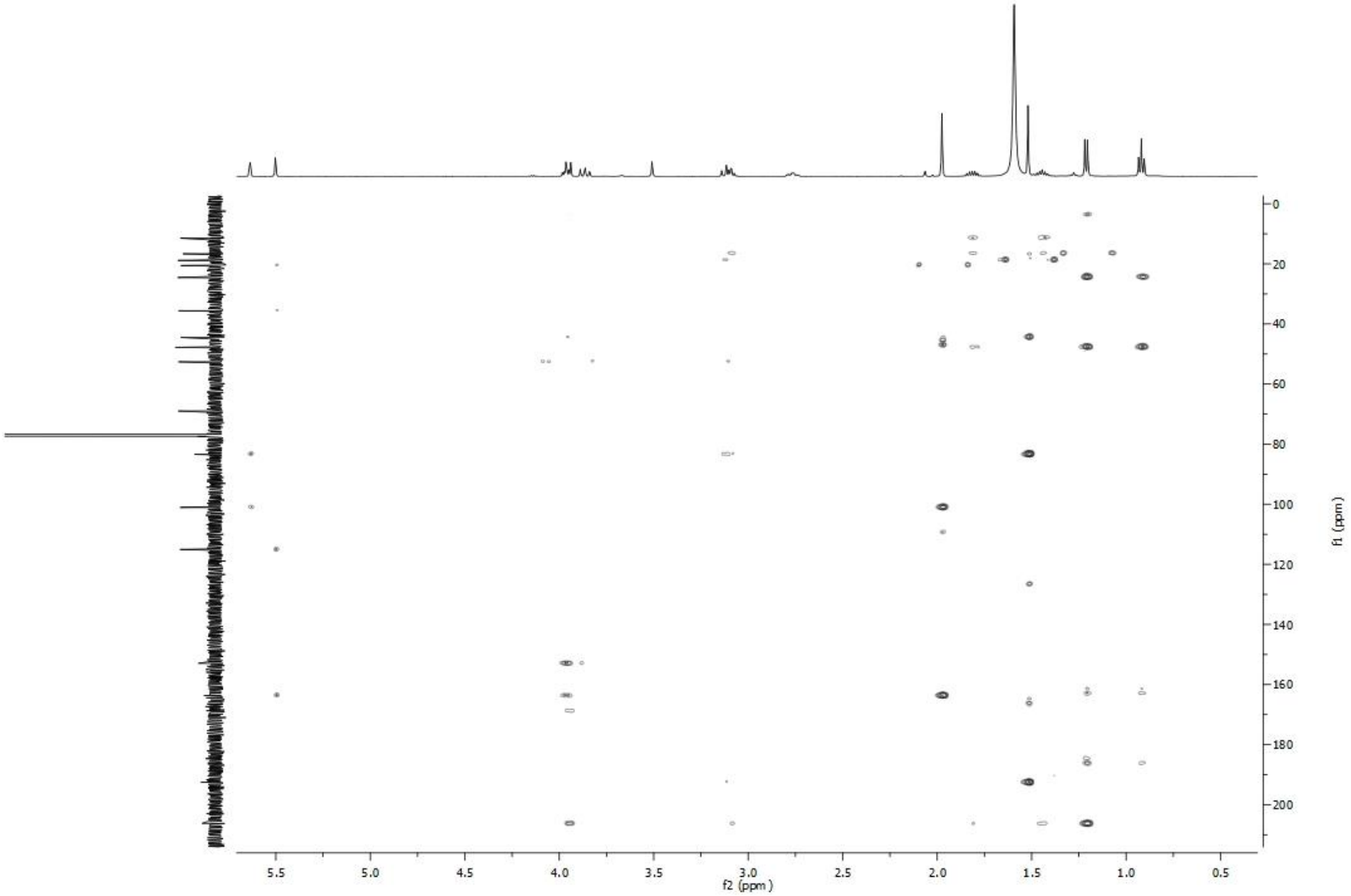

Figure S25. HMBC (500 MHz, $CDCl_3$) spectrum of colletotrichone C (**3**)

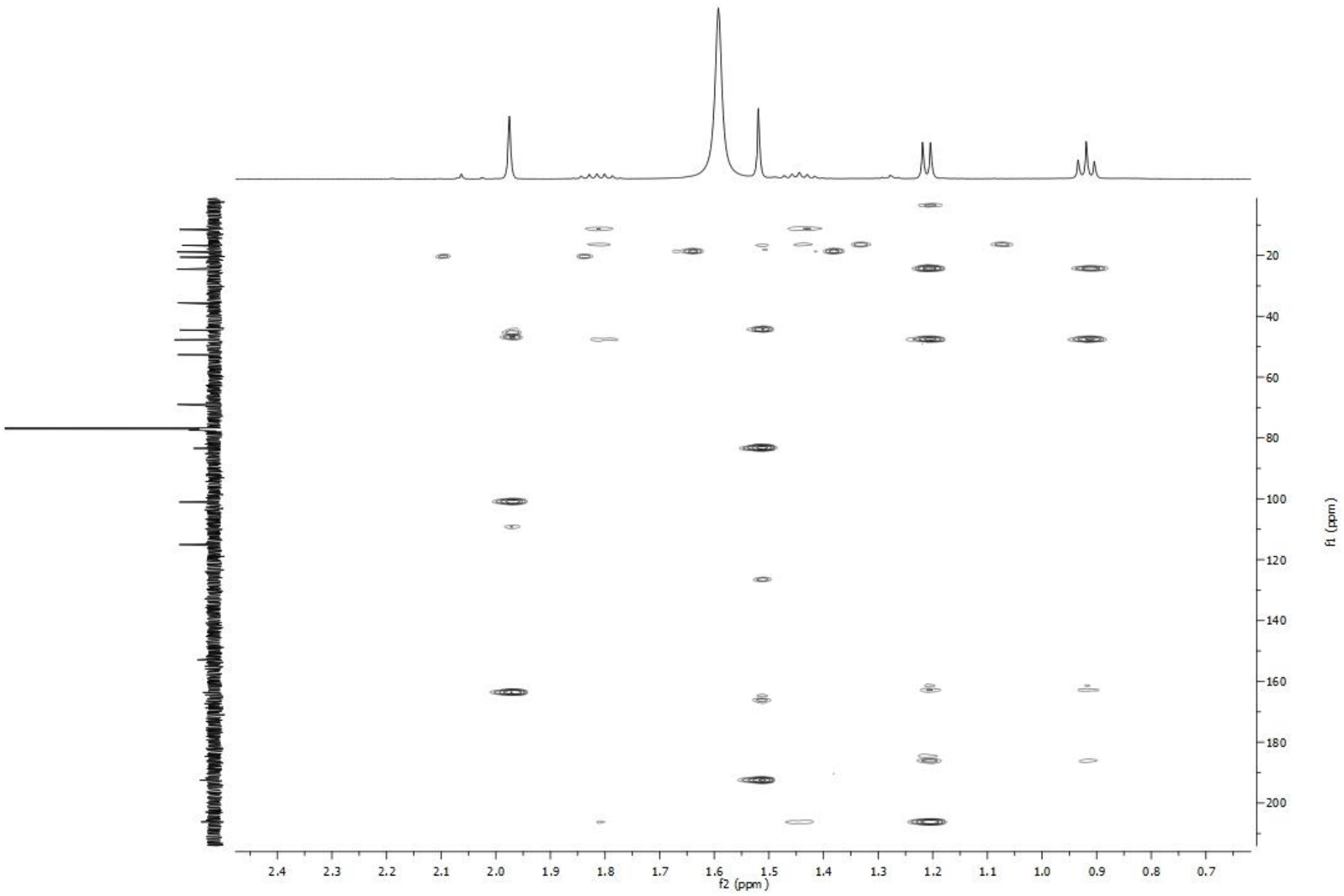

Figure S25. HMBC (500 MHz, $CDCl_3$) spectrum of colletotrichone C (**3**)

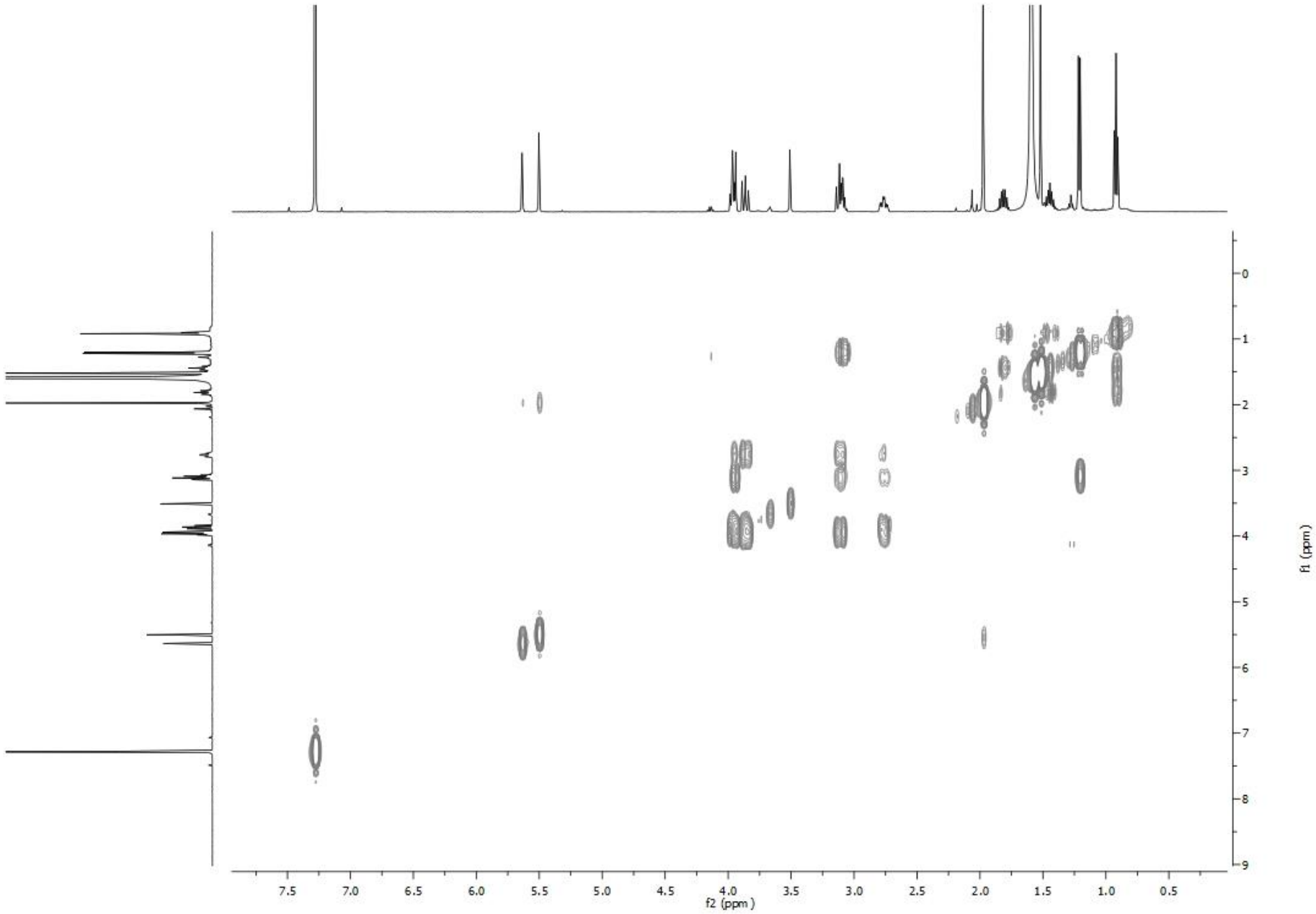

Figure S26. ^{1}H, ^{1}H COSY (500 MHz, $CDCl_3$) spectrum of colletotrichone C (**3**)

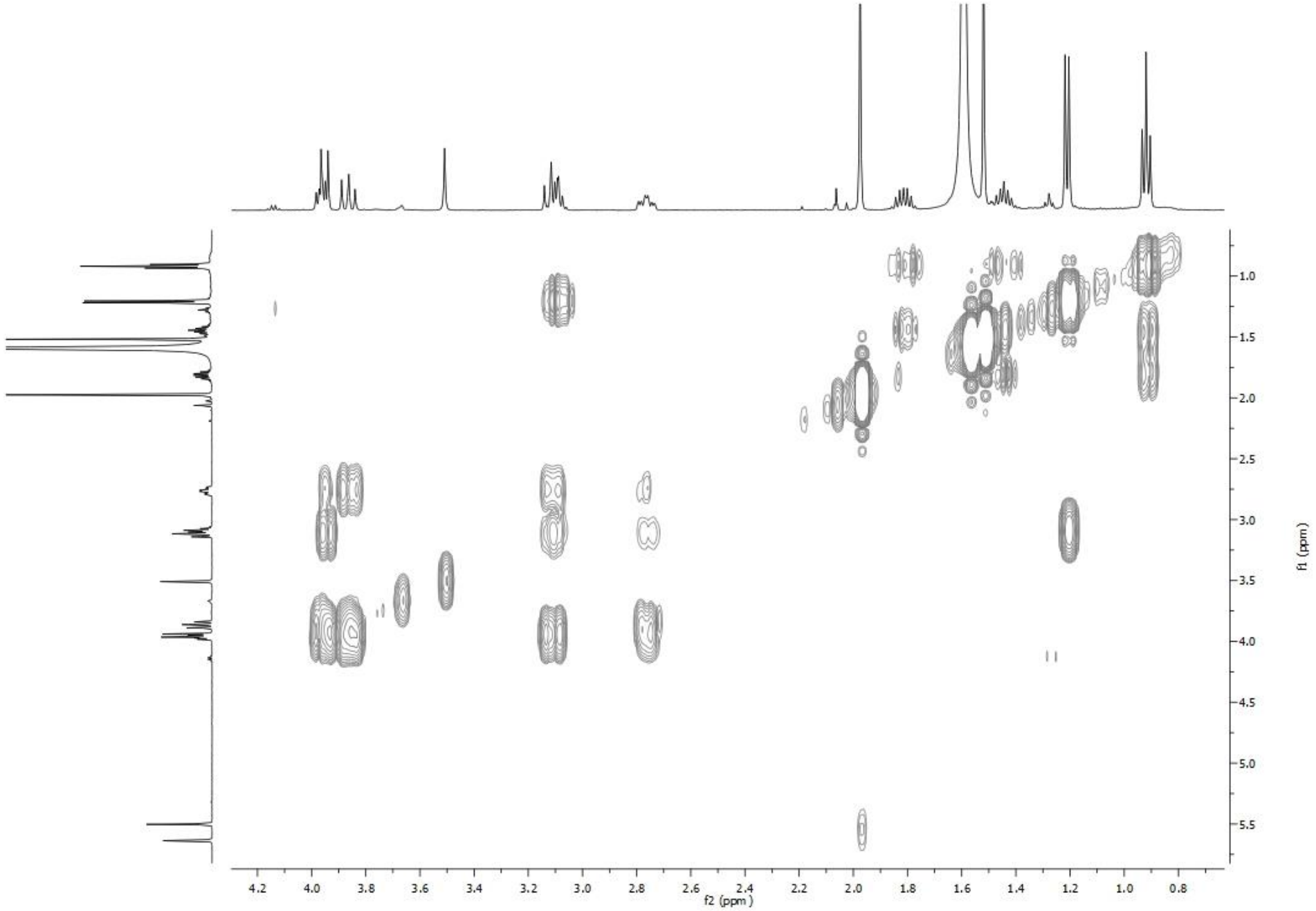

Figure S26. ^{1}H, ^{1}H COSY (500 MHz, $CDCl_3$) spectrum of colletotrichone C (**3**)

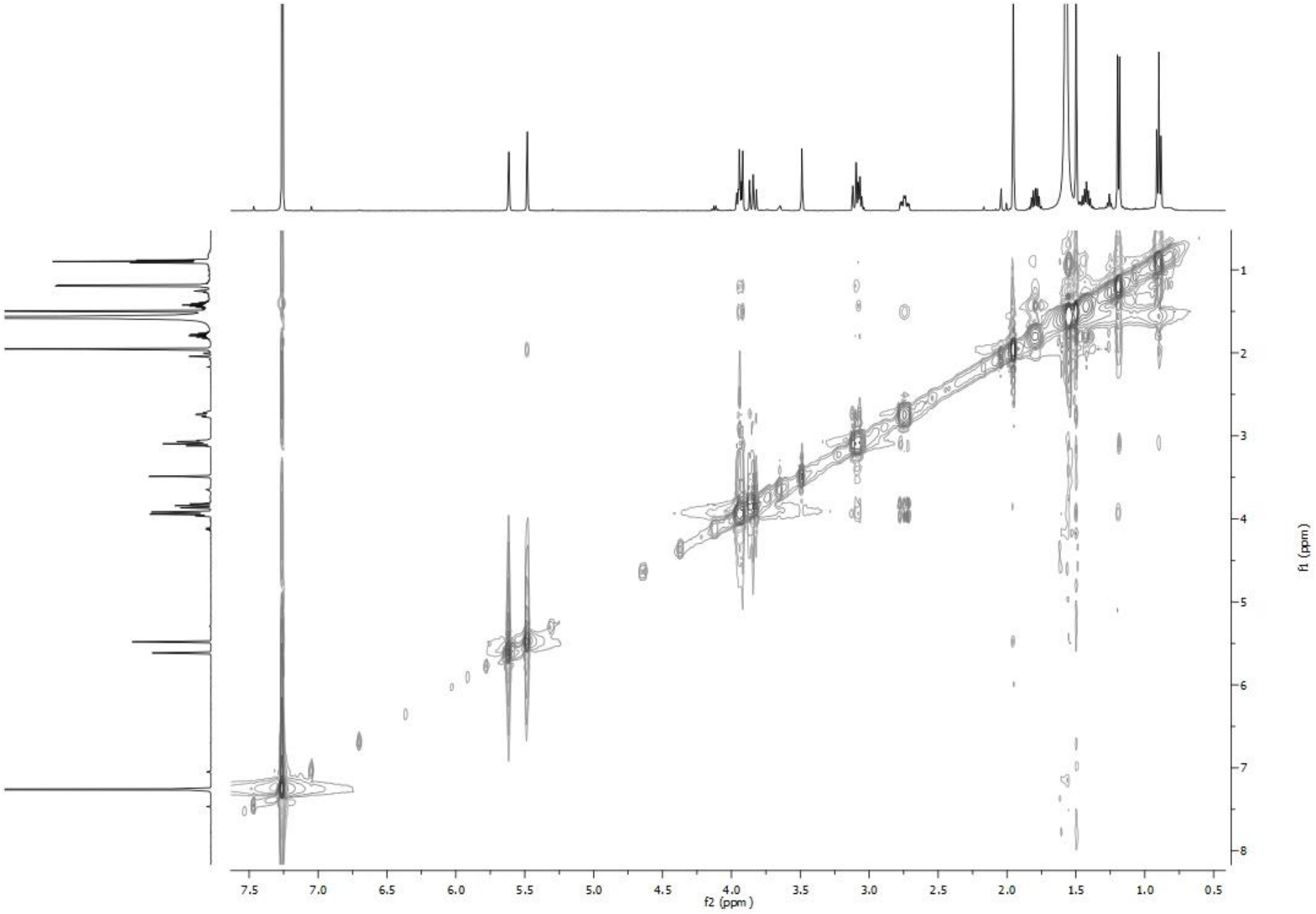

Figure S27. NOESY (500 MHz, $CDCl_3$) spectrum of colletotrichone C (**3**)

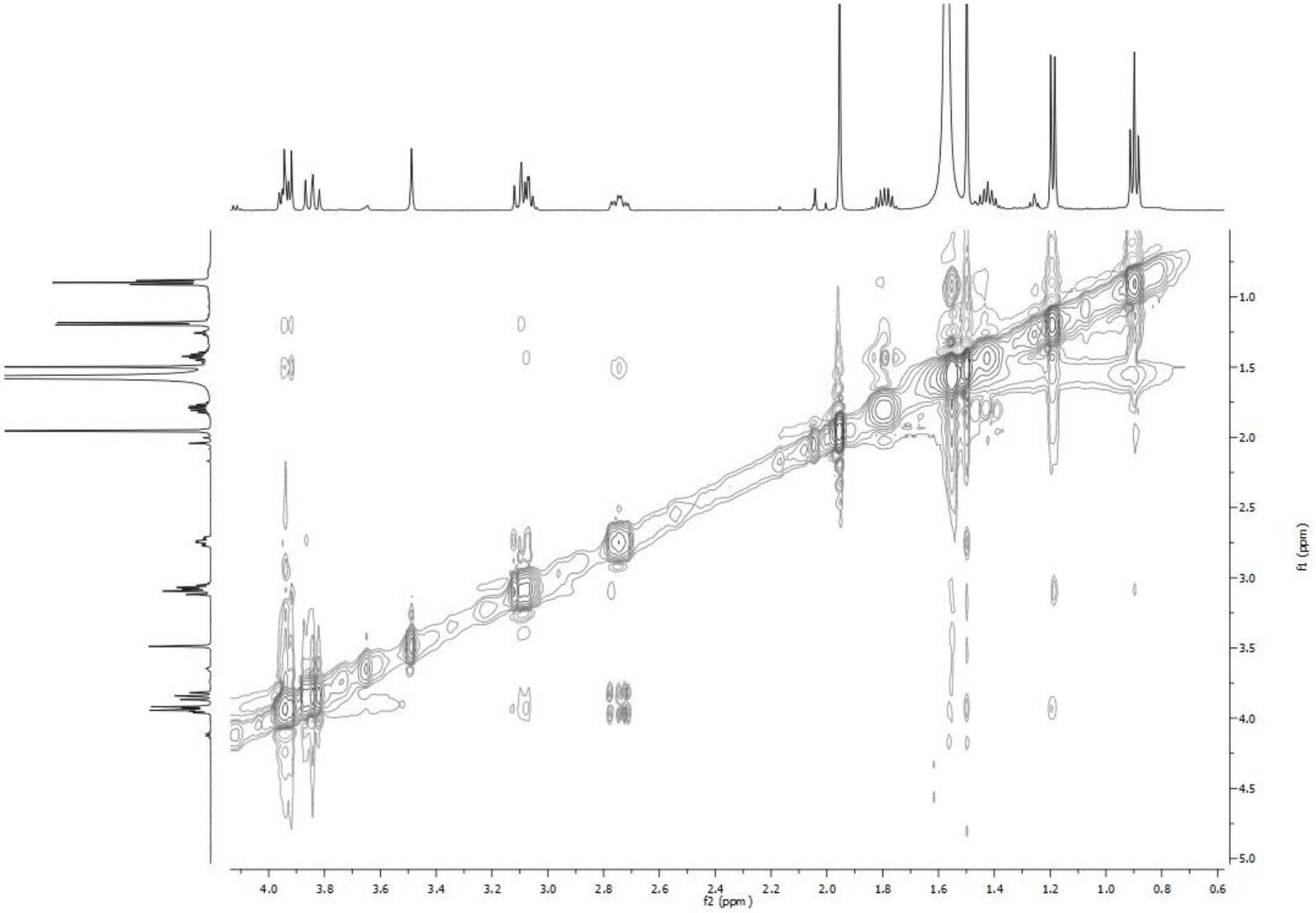

Figure S27. NOESY (500 MHz, $CDCl_3$) spectrum of colletotrichone C (**3**)

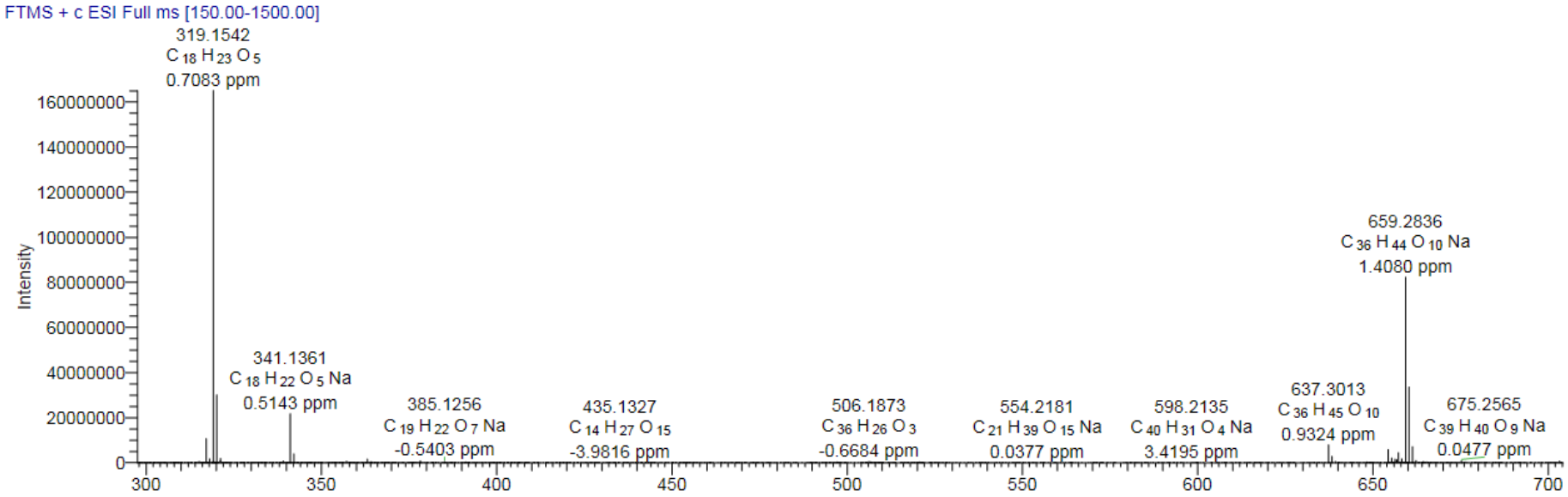

Figure S28. Positive ESIHRMS of colletotrichone C (**3**)

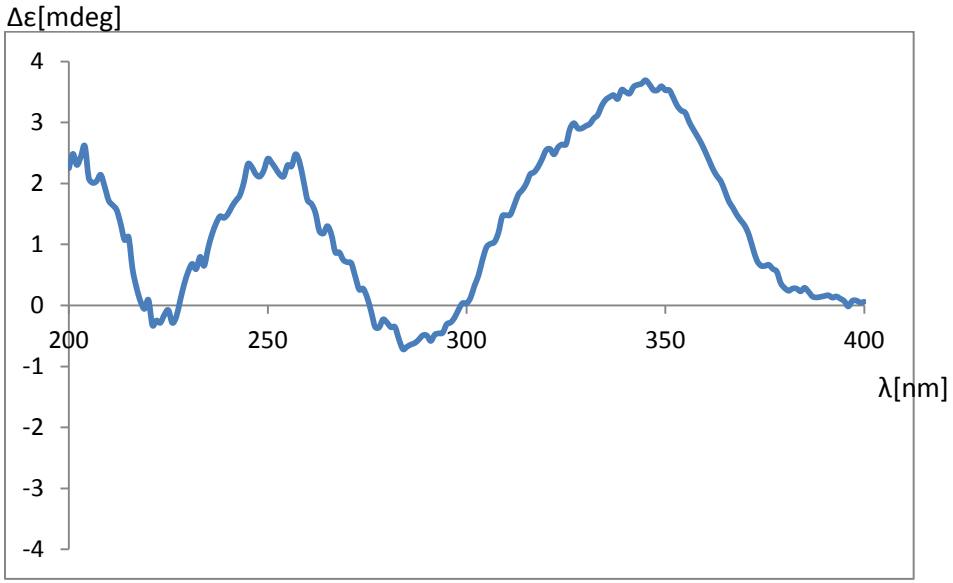

Figure S29. CD spectrum of colletotrichone C (**3**) (0.1 mg/mL, MeOH)

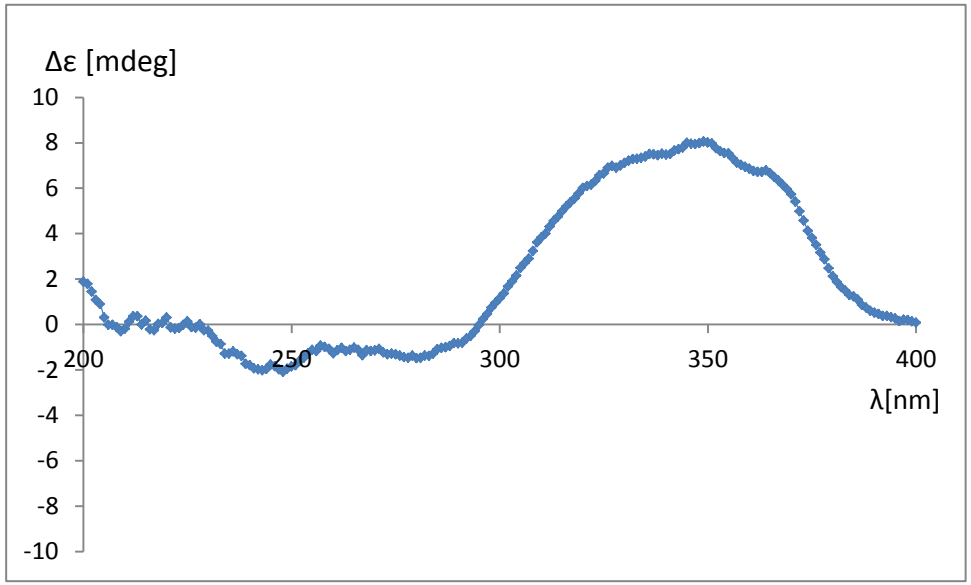

Figure S30. CD spectrum of chermesinone B (**4a**) (0.1 mg/mL, MeOH)

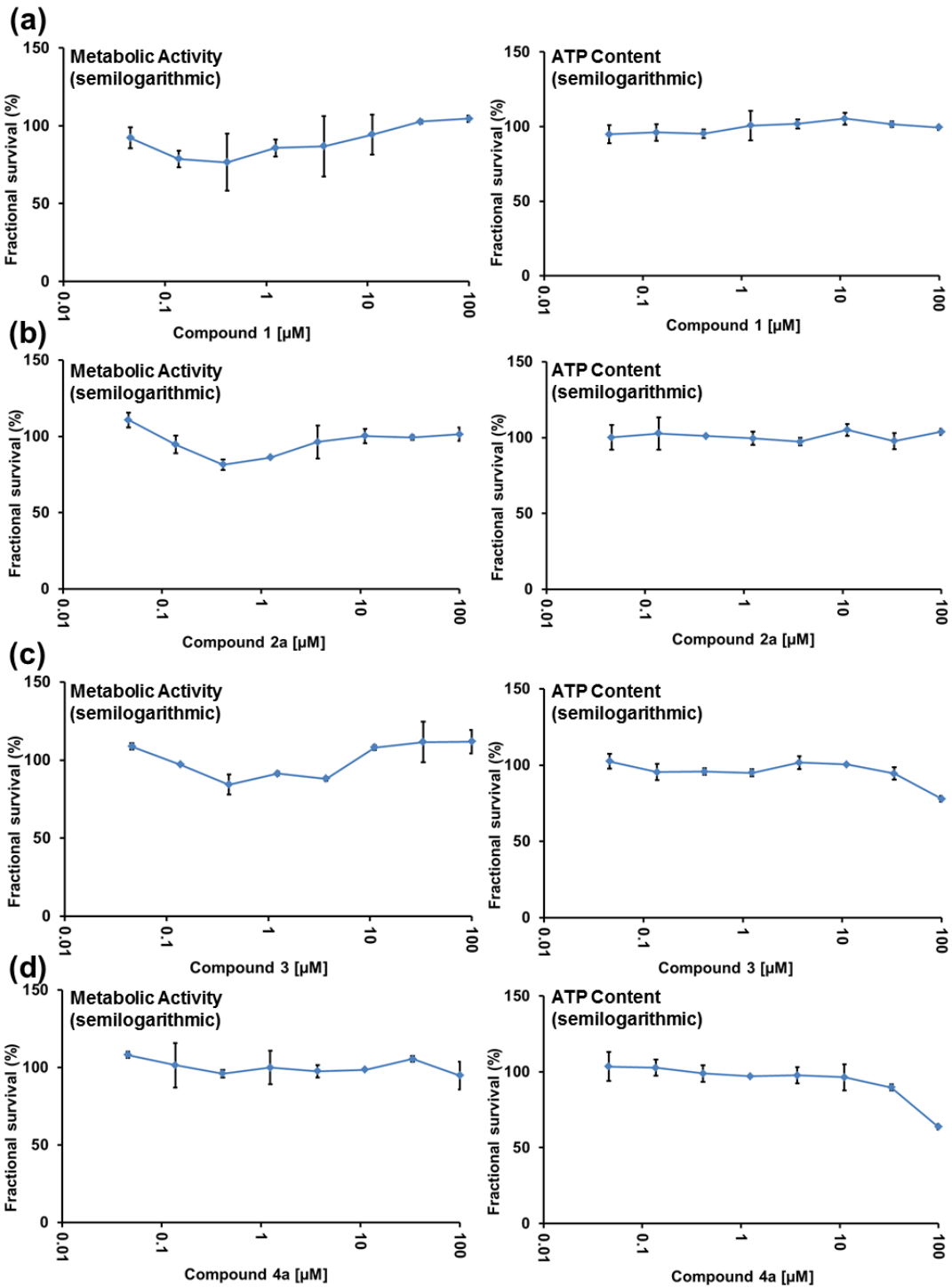

Figure S31. *In vitro* cytotoxic assays of compounds **1**, **2a**, **3** and **4a** against THP-1 cells using a resazurin-based assay (to measure metabolic activity) as well as an ATPlite assay (to measure ATP content). Semilogarithmic representation of the fractional survival (FS in %) of THP-1 cells as a function of concentration is provided.

(a) Compound **1**. (b) Compound **2a**. (c) Compound **3**. (d) Compound **4a**.

Culturing of the THP-1 Cell Line. The human acute monocytic leukemia cell line (THP-1), bearing DSMZ number ACC 16, was used. The THP-1 cells were grown in tissue culture flasks in complete growth medium in an atmosphere of 5% CO_2 and 90% relative humidity in a carbon dioxide incubator. The complete growth medium was prepared by using RPMI-1640 supplemented with 2 mM L-glutamine, 10% FBS, and penicillin (100 IU mL^{-1}, just before use) in double-distilled water. The pH of the medium was adjusted to 7.2, and the medium was sterilized by filtering through 0.2 μm filters in a laminar air flow hood under aseptic conditions.

Subculturing of the THP-1 Cell Line. For subculturing, the medium of the flask having subconfluent growth was changed 1 day in advance. The entire medium from the flask was taken out and discarded. Cells were washed with PBS. Thereafter, 0.5 mL of Trypsin-EDTA in PBS (pre-warmed at 37 °C) was added to make a thin layer on the monolayer of the THP-1 cells. The flask was incubated for approximately 5 min at 37 °C and observed under a microscope. If the cells were found to be detached, complete growth medium (1 mL, pre-warmed at 37 °C) was added to make the cell suspension. An aliquot was taken out and cells were counted and checked for viability with Trypan blue. Cell stock of more than 98% cell viability was accepted for determination of the in vitro cytotoxicity. The cell density was adjusted to 7.5×10^4 cells mL^{-1} by addition of more complete growth medium.

Cytotoxicity assays. A 50 mM stock solution was prepared for each compound (**1**, **2a**, **3** and **4a**) in DMSO and filter-sterilized through 0.2 μm filter under vacuum. From the stock solution, working concentrations were prepared with a dilution factor (DF) of 3 to reach a C_{max} of 100 μM. The *in vitro* cytotoxicity of each compound against the human cancer cell line THP-1 was determined (48 h exposure) using 96-well flat bottom tissue culture plates (black) using two established methods[31] in parallel using a VICTOR multilabel plate reader (PerkinElmer Life And Analytical Sciences, Inc., Boston, MA). The first method consisted of quantification using resazurin (Sigma-Aldrich Chemie GmbH), to measure the mitochondrial activity. The second method consisted of quantification using ATPlite (PerkinElmer Life and Analytical Sciences, Inc.), to measure the available ATP concentration. The final relative viabilities were calculated and represented in percent fractional survival (FS).[1]

Table S1. ^{13}C NMR (125 MHz) and ^{1}H NMR (500 MHz) data of compound **2a** in acetone-d_6

Position	**2a** (acetone-d_6)	
	δ_C	δ_H mult. (J in Hz)
1	146.9	7.38, 1H, s
2	159.1	
3	106.8	6.25, 1H, s
4	105.3	5.28, 1H, br s
5	190.6	
6	82.7	
7	43.4	3.93, 1H, d (12.0)
8	114.5	
9	144.0	
10	55.6	4.36, 1H, d (12.0)
11	206.5	
12	46.7	3.05, 1H, m
13	25.4	1.67, 1H, m
		1.36, 1H, m
14	10.5	0.83, 3H, t (7.4)
15	18.3	2.17, 3H, s
16	22.4	1.51, 3H, s
17	13.5	1.07, 3H, d (6.7)
18	169.5	

Table S2. Boltzmann averaged distances from H-10 to Me-17 and from H-10 to H-12 of four diastereomers of compound **2a** (6*R*,7*R*,10*R*,12*R* (**2c**); 6*R*,7*R*,10*R*,12*S* (**2a**); 6*R*,7*R*,10*S*,12*S* (**2d**); 6*R*,7*R*,10*S*,12*R* (**2b**))[a], calculated on wB97XD/6-311+G(2df,2p) level of theory.

6*R*,7*R*,10*R*,12*R*			Distance (Å)		6*R*,7*R*,10*R*,12*S*			Distance (Å)	
Conformer	ΔG (Hartree)	B-Factor	H-10 to Me-17	H-10 to H-12	Conformer	ΔG (Hartree)	B-Factor	H-10 to Me-17	H-10 to H-12
1	0.00145	0.060484	2.505	2.585	1	0	0.325127	4.258	2.462
2	0	0.278278	2.417	2.605	2	0.001332	0.080012	4.516	3.006
3	0.002852	0.01581	2.343	3.342	3	0.002346	0.027519	4.482	2.585
6	5.9E-05	0.261522	2.824	2.514	4	0.002216	0.031554	4.099	2.634
8	0.002454	0.024037	2.335	3.334	6	0.00235	0.027403	4.483	2.589
10	0.001427	0.061966	2.5	2.589	13	0.000114	0.288364	4.254	2.462
15	3.8E-05	0.267367	2.757	2.515	17	0.000373	0.219555	4.255	2.464
20	0.00142	0.062425	2.497	2.588					
	Weighted average		2.620	2.58372903		Weighted average		4.284	2.518

6*R*,7*R*,10*S*,12*S*			Distance (Å)		6*R*,7*R*,10*S*,12*R*			Distance (Å)	
Conformer	ΔG (Hartree)	B-Factor	H-10 to Me-17	H-10 to H-12	Conformer	ΔG (Hartree)	B-Factor	H-10 to Me-17	H-10 to H-12
1	0.003284	0.014895	2.887	2.559	1	0.002892	0.04132	2.454	2.348
3	0.003339	0.014058	4.258	2.358	2	0.003739	0.016942	4.37	2.363
9	0.001525	0.094874	3.025	3.604	3	0.003056	0.034769	4.087	2.35
10	0	0.472355	3.473	3.636	4	0.004156	0.010923	2.593	2.429
12	0.002321	0.041046	3.379	3.617	9	0	0.86733	4.831	3.633
13	0.000312	0.340129	3.467	3.64	10	0.003904	0.014241	4.775	3.462
	Weighted average		3.426	3.599		Weighted average		4.711	3.525

[a] Only conformers with Boltzmann factor > 0.01 are considered.

In Table S1, we presume that the configuration of C-6 is *R*, and the discussion showed below is useful for the assignment of relative configurations at position C-10 and C-12 of compound **2a**.

For a flexible structure, the distance of each contributing conformer will result in dynamic averaged NOEs, if the interconversion between conformers is rapidly on the NMR time-scale.[2] Therefore, we can use Boltzmann averaged distance to describe the spatial relationship of atoms in compound **2a** for NOESY analysis.

The relationship of interproton distance (r_{IS}) and normalized NOE intensity (η_{IS}) can be described by formulae:[2]

$$\eta_{IS} = \sigma_{IS}\tau_m \qquad \sigma_{IS} = kr_{IS}^{-6}$$

$$k = \left(\frac{\mu_0}{4\pi}\right)\frac{\hbar^2\gamma^4}{10}\left(\frac{6\tau_c}{1+4\omega^2\tau_c^2} - \tau_c\right)$$

When the NOESY measurement was performed **within one experiment**, the *k* and τ_m value can be considered to be **constant** for each spin pair.[2]

Therefore, the distance and NOE intensity can be described in a proportional relationship:[2]

$$\frac{\eta_{I1S}}{\eta_{I2S}} = \frac{r_{I1S}^{-6}}{r_{I2S}^{-6}}$$

From the above, we can conclude which pair of protons has closer distance by comparing the NOE intensities.

From the 2D NOESY spectrum, we can clearly see that there is a cross peak between H-10 and H-12, while no cross peak is observed between H-10 and Me-17, which suggests that **the averaged distance of H-10 and H-12 is smaller than H-10 and Me-17**. Moreover, the absence of cross peak between H-10 and Me-17 indicates the distance between them is larger than the detection limit.

For **6*R*,7*R*,10*R*,12*R*** (**2c**) configuration, the distance from Me-17 to H-10 and the distance from H-10 to H-12 are similar (the difference is only 0.036 Å), and are both smaller than 3 Å, where the NOE can be detected.[3–7]

For **6*R*,7*R*,10*S*,12*S*** (**2d**) configuration, the distances between H-10 and Me-17 is smaller than H-10 and H-12.

It is worth to mention here that the earlier reported compound chermesinone C has 7*S*,10*S*,12*S* configuration (which is also the same relative configuration to 7*R*,10*R*,12*R*), and its H-10 and Me-17 as well as H-10 and H-12 have cross peaks in NOESY spectrum.[8]

Therefore, the two possibilities for compound **2a** are **6*R*,7*R*,10*R*,12*S*** and **6*R*,7*R*,10*S*,12*R*** (or their enantiomers). For the further details, please see Figure 5 in the manuscript.

Table S3. Comparison of ^{1}H and ^{13}C NMR spectroscopic data for compounds **2a**, monochaetin (**4b**),[a] **3**, and chermesinone B (**4a**)[a] ($CDCl_3$)

Position	**2a**		**Monochaetin (4b)**		**3**		**Chermesinone B (4a)**	
	δ_C	δ_H mult. (*J* in Hz)	δ_C	δ_H mult. (*J* in Hz)	δ_C	δ_H mult. (*J* in Hz)	δ_C	δ_H mult. (*J* in Hz)
1	147.2	7.30, 1H, s	143.3	6.79, dd (1.9, 1.3)	69.0	3.95, 1H, dd (11.5, 5.4) 3.84, 1H, dd (13.5, 11.5)	143.5	6.83, s
2	159.4		158.5		163.9		158.8	
3	107.3	6.00, 1H, s	107.0	6.02, q (< 0.4)	101.1	5.48, 1H, br s	107.3	6.05, s
4	105.8	5.36, 1H, br s	105.7	5.29, d (1.3)	115.0	5.62, 1H, br s	106.1	5.34, d (0.8)
5	191.5		191.8		192.5		192.1	
6	83.2		82.6		83.4		82.8	
7	43.0	3.89, 1H, br s	43.7	3.76, dd (12.8, 1.9)	44.5	3.10, 1H, dd (12.5, 11.5)	43.8	3.81, dd (12.9, 1.9)
8	114.6		116.2		35.6	2.74, 1H, dddd (13.5, 11.5, 5.4, 1.5)	116.5	
9	144.5		145.5		153.0		145.7	
10	55.7	3.89, 1H, br s	52.1	4.05, d (12.8)	52.6	3.93, 1H, d (12.5)	51.7	4.09, d (12.9)
11	206.3		205.9		206.2		206.2	
12	46.6	3.10, 1H, m	46.7	3.19, qdd (6.7, 7.4, 5.4)	47.8	3.07, 1H, m	47.3	3.15, m
13	26.2	1.60, 1H, m 1.37, 1H, m	26.3	1.81, qdd (7.4, 13.0, 5.4) 1.48, qdd (7.4, 13.0, 7.4)	24.5	1.79, 1H, m 1.42, 1H, m	25.1	1.80, m 1.43, m
14	11.1	0.81, 3H, t (7.4)	11.5	0.97, t (7.4)	11.5	0.90, 3H, t (7.5)	11.7	0.90, t (7.4)
15	19.5	2.14, 3H, s	19.5	2.13, d (< 0.4)	20.6	1.95, 3H, s	19.8	2.17, s
16	23.2	1.57, 3H, s	18.9	1.32, s	18.8	1.50, 3H, s	19.1	1.36, s
17	**14.1**	**1.09, 3H, d (6.5)**	**14.4**	**1.11, d (6.7)**	**16.7**	**1.19, 3H, d (7.2)**	**17.1**	**1.24, d (7.1)**
18	168.6		169.1		168.8		169.3	

[a] Adapted from the Supporting Information of Huang *et al.* (2011).[8]

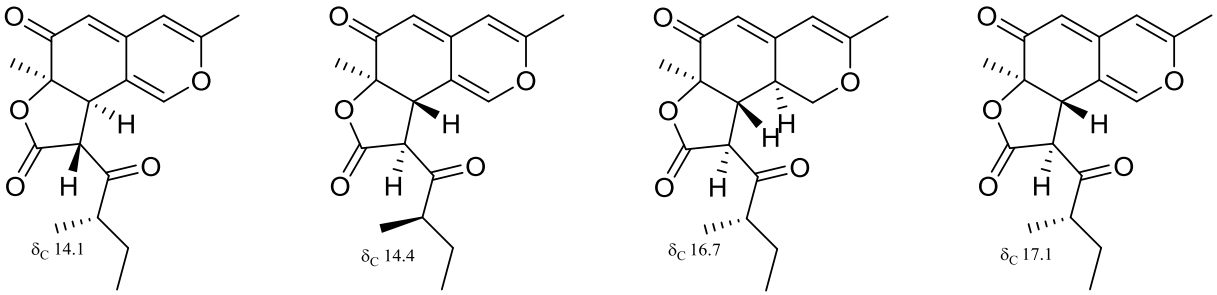

2a Monochaetin **4b** **3** Chermesinone B **4a**

Huang *et al.* (2011) had compared the chemical shifts of monochaetin (**4b**) and chermesinone B (**4a**), and concluded that different relative configurations of C-10 and C-12 lead to different chemical shifts of Me-17.[8] On one hand, the chemical shifts of Me-17 of **2a** are close to compound monochaetin (**4b**), which suggests that the Me-17 and H-10 of compound **2a** have opposite orientation like monochaetin (**4b**). On the other hand, Me-17 of compound **3** showed close chemical shifts to compound chermesinone B (**4a**), which indicates the relative orientation of Me-17 and H-10 is the same as chermesinone B (**4a**).

Table S4. Experimental ^{13}C NMR data ($CDCl_3$) of colletotrichone B (**2a**) and calculated ^{13}C NMR data[a] of compounds **2a**/**2b**/**2c**/**2d**

Atom No.	Exp data of **2a**	Cacld **2a** (6*R*,7*R*,10*R*,12*S*)	Abs deviation	Cacld **2b** (6*R*,7*R*,10*S*,12*R*)	Abs deviation	Cacld **2c** (6*R*,7*R*,10*R*,12*R*)	Abs deviation	Cacld **2d** (6*R*,7*R*,10*S*,12*S*)	Abs deviation
1	147.2	146.84	0.36	147.08	0.12	147.15	0.05	147.60	0.40
2	159.4	157.51	1.89	158.25	1.15	157.97	1.43	158.52	0.88
3	107.3	109.37	2.07	110.75	3.45	110.47	3.17	110.68	3.38
4	105.8	107.40	1.60	108.05	2.25	107.06	1.26	108.45	2.65
5	191.5	189.83	1.67	190.62	0.88	189.99	1.51	191.62	0.12
6	83.2	80.72	2.48	81.88	1.32	80.50	2.70	81.81	1.39
7	43.0	42.42	0.58	48.72	5.72	42.27	0.73	48.90	5.90
8	114.6	117.26	2.66	116.72	2.12	118.05	3.45	116.56	1.96
9	144.5	138.69	5.81	142.61	1.89	140.14	4.36	142.55	1.95
10	55.7	56.59	0.89	59.44	3.74	55.48	0.22	59.65	3.95
11	206.3	213.03	6.73	207.09	0.79	212.45	6.15	210.39	4.09
12	46.6	45.67	0.93	47.58	0.98	46.47	0.13	47.48	0.88
13	26.2	29.11	2.91	27.83	1.63	25.09	1.11	27.96	1.76
14	11.1	12.00	0.90	13.31	2.21	12.08	0.98	12.00	0.90
15	19.5	18.18	1.32	19.12	0.38	19.18	0.32	19.12	0.38
16	23.2	22.70	0.50	24.75	1.55	23.82	0.62	24.85	1.65
17	**14.1**	**15.35**	**1.25**	**15.77**	**1.67**	**16.31**	**2.21**	**18.74**	**4.64**
18	168.6	167.58	1.02	170.77	2.17	167.85	0.75	170.61	2.01

[a] The conformer distributions of the molecules in question were searched in a systematic approach with the MMFF routine of Spartan'14 (Wavefunction, Inc.: Irvine, CA, 2014).[9] The geometries of all resulting conformers within an energy range of < 25 kJ/mol above the global minimum were then optimized, first with HF/3-21G and then within < 15 kJ/mol by DFT using the wB97X-D functional and the 6-31G* basis set. The resulting geometries with preliminary Boltzmann factors > 0.001 were used without further geometry optimization to calculate the NMR spectra with EDF2/6-31G*; SPARTAN's corrected shifts were used without further solvent corrections (the solvent model is not yet provided in Spartan'14) . The final Boltzmann factors were obtained with wB97XD/6-311+G(2df,2p), using Gaussian g09.[10] The NMR shifts of all remaining conformers were averaged with respect to their final Boltzmann factors.

Table S5. Experimental/calculated ^{13}C NMR data ($CDCl_3$) of chermesinone B (**4a**) and monochaetin (**4b**)[a]

Atom No.	**4a** Exp. data	**4a** Calc. data	Abs deviation	**4b** Exp. data	**4b** Calc. data	Abs deviation
1	143.5	144.5	1.0	143.3	143.4	0.1
2	158.8	157.7	1.1	158.5	156.6	1.9
3	107.3	110.1	2.8	107.0	107.4	0.4
4	106.1	107.7	1.6	105.7	107.9	2.2
5	192.1	189.8	2.3	191.8	189.4	2.4
6	82.8	82.0	0.8	82.6	82.2	0.3
7	43.8	43.4	0.4	43.7	43.4	0.3
8	116.5	119.8	3.3	116.2	117.6	1.4
9	145.7	141.7	4.0	145.5	139.8	5.7
10	51.7	54.1	2.4	52.1	51.0	1.1
11	206.2	214.1	7.9	205.9	211.0	5.1
12	47.3	45.6	1.7	46.7	44.1	2.6
13	25.1	28.2	3.1	26.3	26.0	0.3
14	11.7	12.4	0.7	11.5	8.9	2.6
15	19.8	19.4	0.4	19.5	17.3	2.2
16	19.1	18.9	0.2	18.9	17.8	1.1
17	**17.1**	**18.9**	**1.8**	**14.4**	**13.4**	**1.0**
18	169.3	170.5	1.2	169.1	169.4	0.3

[a] The conformer distributions of the molecules in question were searched in a systematic approach with the MMFF routine of Spartan'14 (Wavefunction, Inc.: Irvine, CA, 2014).[9] The geometries of all resulting conformers within an energy range of < 25 kJ/mol above the global minimum were then optimized, first with HF/3-21G and then within < 15 kJ/mol by DFT using the wB97X-D functional and the 6-31G* basis set. The resulting geometries with preliminary Boltzmann factors > 0.001 were used without further geometry optimization to calculate the NMR spectra with EDF2/6-31G*; SPARTAN's corrected shifts were used without further solvent corrections (the solvent model is not yet provided in Spartan'14) . The final Boltzmann factors were obtained with wB97XD/6-311+G(2df,2p), using Gaussian g09.[10] The NMR shifts of all remaining conformers were averaged with respect to their final Boltzmann factors.

References

(1) Kusari, S.; Zühlke, S.; Kosuth, J.; Cellarova, E.; Spiteller, M., *J. Nat. Prod.* **2009**, 72, 1825–1835.

(2) Jones, C. R.; Butts, C. P.; Harvey, J. N. *Beilstein J. Org. Chem.* **2011**, *7*, 145–150.

(3) Yen, W.-H.; Hu, L.-C.; Su, J.-H.; Lu, M.-C.; Twan, W.-H.; Yang, S.-Y.; Kuo, Y.-C.; Weng, C.-F.; Lee, C.-H.; Kuo, Y.-H.; Sung, P.-J. *Molecules* **2012**, *17*, 14058–14066.

(4) Su, Y.-D.; Su, T.-R.; Wen, Z.-H.; Hwang, T.-L.; Fang, L.-S.; Chen, J.-J.; Wu, Y.-C.; Sheu, J.-H.; Sung, P.-J. *Mar. Drugs* **2015**, *13*, 1037–1050.

(5) Maslovskaya, L. A.; Savchenko, A. I.; Pierce, C. J.; Gordon, V. A.; Reddell, P. W.; Parsons, P. G.; Williams, C. M. *Chem. Eur. J.* **2014**, *20*, 14226–14230.

(6) Wu, S.-B.; Bao, Q.-Y.; Wang, W.-X.; Zhao, Y.; Xia, G.; Zhao, Z.; Zeng, H.; Hu, J.-F. *Planta Med.* **2011**, *77*, 922–928.

(7) Jiao, W.; Blunt, J. W.; Cole, A. L. J.; Munro, M. H. G. *J. Nat. Prod.* **2004**, *67*, 1434–1437.

(8) Huang, H.; Feng, X.; Xiao, Z.; Liu, L.; Li, H.; Ma, L.; Lu, Y.; Ju, J.; She, Z.; Lin, Y. *J. Nat. Prod.* **2011**, *74*, 997−1002.

(9) Shao, Y.; Molnar, L. F.; Jung, Y.; Kussmann, J.; Ochsenfeld, C.; Brown, S. T.; Gilbert, A. T. B.; Slipchenko, L. V.; Levchenko, S. V.; O'Neill, D. P.; DiStasio, Jr. R. A.; Lochan, R. C.; Wang, T.; Beran, G. J. O.; Besley, N. A.; Herbert, J. M.; Lin, C. Y.; Van Voorhis, T.; Chien, S. H.; Sodt, A.; Steele, R. P.; Rassolov, V. A.; Maslen, P. E.; Korambath, P. P.; Adamson, R. D.; Austin, B.; Baker, J.; Byrd, E. F. C.; Dachsel, H.; Doerksen, R. J.; Dreuw, A.; Dunietz, B. D.; Dutoi, A. D.; Furlani, T. R.; Gwaltney, S. R.; Heyden, A.; Hirata, S.; Hsu, C-P.; Kedziora, G.; Khalliulin, R. Z.; Klunzinger, P.; Lee, A. M.; Lee, M. S.; Liang, W. Z.; Lotan, I.; Nair, N.; Peters, B.; Proynov, E. I.; Pieniazek, P. A.; Rhee, Y. M.; Ritchie, J.; Rosta, E.; Sherrill, C. D.; Simmonett, A. C.; Subotnik, J. E.; Woodcock III, H. L.; Zhang, W.; Bell, A. T.; Chakraborty, A. K.; Chipman, D. M.; Keil, F. J.; Warshel, A.; Hehre, W. J.; Schaefer, H. F.; Kong, J.; Krylov, A. I.; Gill P. M. W.; Head-Gordon, M. *Phys. Chem. Chem. Phys.* **2006**, *8*, 3172.

(10) Frisch, M. J.; Trucks, G. W.; Schlegel, H. B.; Scuseria, G. E.; Robb, M. A.; Cheeseman, J. R.; Scalmani, G.; Barone, V.; Mennucci, B.; Petersson, G. A.; Nakatsuji, H.; Caricato, M.; Li, X.; Hratchian, H. P.; Izmaylov, A. F.; Bloino, J.; Zheng, G.; Sonnenberg, J. L.; Hada, M.; Ehara, M.; Toyota, K.; Fukuda, R.; Hasegawa, J.; Ishida, M.; Nakajima, T.; Honda, Y.; Kitao, O.; Nakai, H.; Vreven, T.; Montgomery, J. A.; Peralta, J. E.; Ogliaro, F.; Bearpark, M.; Heyd, J. J.; Brothers, E.; Kudin, K. N.; Staroverov, V. N.; Kobayashi, R.; Normand, J.; Raghavachari, K.; Rendell, A.; Burant, J. C.; Iyengar, S. S.; Tomasi, J.; Cossi, M.; Rega, N.; Millam, J. M.; Klene, M.; Knox, J. E.; Cross, J. B.; Bakken, V.; Adamo, C.; Jaramillo, J.; Gomperts, R.; Stratmann, R. E.; Yazyev, O.; Austin, A. J.; Cammi, R.; Pomelli, C.; Ochterski, J. W.; Martin, R. L.; Morokuma, K.; Zakrzewski, V. G.; Voth, G. A.; Salvador, P.; Dannenberg, J. J.; Dapprich, S.; Daniels, A. D.; Farkas, O.; Foresman, J. B.; Ortiz, J. V.; Cioslowski, J.; Fox, D. J. Gaussian 09W, Version 7.0; Gaussian: Wallingford, CT, 2009.